



# **Supporting Information:**

## **Headgroup Structure and Cation Binding in**

## **Phosphatidylserine Lipid Bilayers**

Hanne Antila,<sup>†</sup> Pavel Buslaev,<sup>‡</sup> Fernando Favela-Rosales,<sup>¶</sup> Tiago M. Ferreira,<sup>§</sup>  
Ivan Gushchin,<sup>‡</sup> Matti Javanainen,<sup>||</sup> Batuhan Kav,<sup>†</sup> Jesper J. Madsen,<sup>⊥</sup> Josef  
Melcr,<sup>||</sup> Markus Miettinen,<sup>†</sup> Ricky Nencini,<sup>||</sup> O. H. Samuli Ollila,<sup>\*,||</sup> and Thomas J.  
Piggot<sup>△</sup>

<sup>†</sup>*Department of Theory and Bio-Systems, Max Planck Institute of Colloids and Interfaces,  
14424 Potsdam, Germany*

<sup>‡</sup>*Moscow Institute of Physics and Technology, Dolgoprudny, Russia*

<sup>¶</sup>*Departamento de Investigación, Tecnológico Nacional de México, Campus Zacatecas  
Occidente, México*

<sup>§</sup>*NMR group - Institute for Physics, Martin-Luther University Halle-Wittenberg*

<sup>||</sup>*Institute of Organic Chemistry and Biochemistry of the Czech Academy of Sciences,  
Flemingovo nám. 542/2, CZ-16610 Prague 6, Czech Republic*

<sup>⊥</sup>*Department of Chemistry, The University of Chicago, Chicago, Illinois, United States of  
America*

<sup>#</sup>*Department of Global Health, College of Public Health, University of South Florida, Tampa,  
Florida, United States of America*

<sup>@</sup>*Institute of Biotechnology, University of Helsinki*

<sup>△</sup>*Chemistry, University of Southampton, Highfield, Southampton SO17 1BJ, U.K*

E-mail: samuli.ollila@helsinki.fi

# S1 Simulated systems

## S1.1 CHARMM36

*POPC bilayer.* Previously published values<sup>24</sup> calculated from the data available from Ref. 25 are used.

*DOPS and POPS bilayers.* Starting structures for CHARMM36 DOPS and POPS simulations were constructed using the CHARMM-GUI webserver.<sup>26,27</sup> The systems contained a total of 128 lipids (64 per leaflet of the membrane), 35 waters per lipid, and 128 Na<sup>+</sup> ions. Force field parameters for DOPS and POPS were taken from Venable et al. and included the modified parameters for interactions with Na<sup>+</sup> ions.<sup>3</sup> Water was treated using the CHARMM TIP3P model.<sup>28,29</sup> For POPS, an identical system was also constructed in which the 128 Na<sup>+</sup> ions were replaced with 128 K<sup>+</sup> ions.

Simulations of these systems were performed for 500 ns using GROMACS, version 5.0.6.<sup>30</sup> A 2 fs timestep was applied during the simulations, and the LINCS algorithm was used to constrain all bonds to hydrogen atoms.<sup>31,32</sup> For each of the DOPS and POPS systems, two simulations were performed using different randomly assigned starting velocities. The simulations were maintained at temperatures of 303 K and 298 K for DOPS and POPS respectively using the Nosé–Hoover thermostat<sup>33,34</sup> with a coupling constant of 1 ps. A pressure of 1 bar was maintained using the Parrinello–Rahman<sup>35</sup> method with a coupling constant of 5 ps. Pressure coupling was applied in a semi-isotropic manner with the *x* and *y* dimensions, in the plane of the bilayer, fluctuating independently of the *z* dimension. Standard CHARMM36 force field methods were applied for the simulation cut-offs: van der Waals interactions were truncated at 1.2 nm with the interactions switched off between 1.0 nm and 1.2 nm; Coulombic interactions were truncated at 1.2 nm with long-range interactions treated using PME.<sup>36,37</sup>

Analyses on these simulations was performed on the final 100 ns of the simulations.

*POPC:POPS mixtures without additional ions* Simulations of POPC:POPS (5:1) mixtures

**Table S1:** The list of POPC:POPS mixtures simulated with different amounts of added monovalent ions. The salt concentrations are calculated as  $[\text{salt}] = N_c \times [\text{water}] / N_w$ , where  $[\text{water}] = 55.5 \text{ M}$ . This corresponds the concentration in buffer before solvating lipids, which are reported in the experiments by Roux et al.<sup>1</sup>

lipid/counter-ions	force field for lipids / ions	<sup>a</sup> C <sub>ci</sub> (M)	<sup>b</sup> N <sub>i</sub>	<sup>c</sup> N <sub>w</sub>	<sup>d</sup> N <sub>c</sub>	<sup>e</sup> T (K)	<sup>f</sup> t <sub>sim</sub> (ns)	<sup>g</sup> t <sub>anal</sub> (ns)	<sup>h</sup> files
POPC:POPS (5:1)/K <sup>+</sup>	CHARMM36 <sup>2,3</sup>	0	250:50	11207	0	298	200	180	4
POPC:POPS (5:1)/K <sup>+</sup>	CHARMM36 <sup>2,3</sup>	0	110:22	4620	0	298	500	100	5
POPC:POPS (5:1)/K <sup>+</sup>	CHARMM36 <sup>2,3</sup>	0.45	110:22	4926	40	298	200	150	6
POPC:POPS (5:1)/K <sup>+</sup>	CHARMM36 <sup>2,3</sup>	0.89	110:22	4946	79	298	200	150	7
POPC:POPS (5:1)/Na <sup>+</sup>	CHARMM36 <sup>2,3</sup>	0	110:22	4620	0	298	500	100	8
POPC:POPS (5:1)/Na <sup>+</sup>	CHARMM36 <sup>2,3</sup>	0.44	110:22	4965	39	298	200	150	9
POPC:POPS (5:1)/Na <sup>+</sup>	CHARMM36 <sup>2,3</sup>	0.89	110:22	4932	79	298	200	150	10
POPC:POPS (5:1)/K <sup>+</sup>	MacRog <sup>11</sup>	0	120:24	5760	0	298	400	250	12
POPC:POPS (5:1)/K <sup>+</sup>	MacRog <sup>11</sup>	0.50	120:24	5760	52	298	300	200	13
POPC:POPS (5:1)/K <sup>+</sup>	MacRog <sup>11</sup>	1.00	120:24	5760	104	298	300	200	13
POPC:POPS (5:1)/K <sup>+</sup>	MacRog <sup>11</sup>	2.00	120:24	5760	208	298	300	200	13
POPC:POPS (5:1)/K <sup>+</sup>	MacRog <sup>11</sup>	3.00	120:24	5760	311	298	300	200	13
POPC:POPS (5:1)/K <sup>+</sup>	Lipid14/17 <sup>14,15</sup>	0	120:24	5760	0	298	500	200	16
POPC:POPS (5:1)/K <sup>+</sup>	Lipid14/17 <sup>14,15</sup>	0.50	120:24	5760	54	298	300	200	17
POPC:POPS (5:1)/K <sup>+</sup>	Lipid14/17 <sup>14,15</sup>	1.00	120:24	5760	104	298	300	200	17
POPC:POPS (5:1)/K <sup>+</sup>	Lipid14/17 <sup>14,15</sup>	2.00	120:24	5760	208	298	300	200	17
POPC:POPS (5:1)/K <sup>+</sup>	Lipid14/17 <sup>14,15</sup>	3.00	120:24	5760	311	298	300	200	17
POPC:POPS (5:1)/K <sup>+</sup>	Lipid14/17 <sup>14,15</sup>	4.00	120:24	5760	415	298	300	200	17
POPC:POPS (5:1)/Na <sup>+</sup>	Lipid14/17 <sup>14,15</sup>	0	120:24	5760	0	298	500	200	18
POPC:POPS (5:1)/Na <sup>+</sup>	Lipid14/17 <sup>14,15</sup>	0.50	120:24	5760	54	298	300	200	19
POPC:POPS (5:1)/Na <sup>+</sup>	Lipid14/17 <sup>14,15</sup>	1.00	120:24	5760	104	298	300	200	19
POPC:POPS (5:1)/Na <sup>+</sup>	Lipid14/17 <sup>14,15</sup>	2.00	120:24	5760	208	298	300	200	19
POPC:POPS (5:1)/Na <sup>+</sup>	Lipid14/17 <sup>14,15</sup>	3.00	120:24	5760	311	298	300	200	19
POPC:POPS (5:1)/Na <sup>+</sup>	Lipid14/17 <sup>14,15</sup>	4.00	120:24	5760	415	298	300	200	19
POPC:POPS (4:1)/Na <sup>+</sup>	Berger <sup>20,21</sup>	0	102:26	4290	0	310	120	80	22
POPC:POPS (4:1)/Na <sup>+</sup>	Berger <sup>20,21</sup>	1.03	102:26	4290	80	310	200	50	23

<sup>a</sup>Excess Na<sup>+</sup> or K<sup>+</sup> concentration

<sup>b</sup>Number of lipid molecules with largest mole fraction

<sup>c</sup>Number of water molecules

<sup>d</sup>Number of additional cations

<sup>e</sup>Simulation temperature

<sup>f</sup>Total simulation time

<sup>g</sup>Time used for analyses

<sup>h</sup>Reference for simulation files

containing a total of 132 lipids (110 POPC and 22 POPS) were constructed using the CHARMM-GUI.<sup>26,27</sup> Two identical systems were constructed, apart from one system was neutralised through the addition of 22 Na<sup>+</sup> ions while the other system contained 22 K<sup>+</sup> ions. As per the pure POPS CHARMM36 simulations, 35 water per lipid were added. All other system and simulation parameters and settings were identical to those used in the CHARMM36 POPS simulations.

Simulations of POPC:POPS (5:1) and POPC:POPS (1:1) mixtures containing total 300 lipids (250:50 and 150:150, respectively) with neutralizing potassium counterions were prepared using the CHARMM-GUI.<sup>26,27</sup> The systems were simulated using Gromacs 5<sup>30</sup> and CHARMM36 force field with the simulation parameters given by the CHARMM-GUI at 298 K. For further details see table S1.

*POPC:POPS (5:1) mixtures with additional monovalent ions.* POPC:POPS (110:22) mixtures containing total 132 lipids with the additional potassium or sodium ions corresponding concentrations of ~450 mM and 890 mM were generated with the CHARMM-GUI.<sup>26,27</sup> Systems were simulated using Gromacs 5<sup>30</sup> and CHARMM36 force field with the simulation parameters given by the CHARMM-GUI at 298 K. For further details, simulation files and data, see table S1 and Refs. 6,7,9,10.

*POPC:POPS (5:1) mixtures with additional calcium using NBfix1 parameters.* POPC:POPS (5:1) mixtures containing total 300 (250:50) lipids and 0.26 M and 1 M CaCl<sub>2</sub> were prepared using the CHARMM-GUI in January 2018.<sup>26,27</sup> The ion parameters generated by CHARMM-GUI at the time are labeled here as NBfix1.<sup>38</sup> Systems were simulated using Gromacs 5<sup>30</sup> and CHARMM36 force field with the simulation parameters given by the CHARMM-GUI at 298 K.

*POPC:POPS (5:1) mixtures with additional calcium using NBfix1 parameters.* **Ricky, please update the simulation methods.** Systems were prepared using the CHARMM-GUI in August

2019.<sup>26,27</sup> The ion parameters generated by CHARMM-GUI at the time are labeled here as NBfix2.<sup>39</sup>

## S1.2 CHARMM36ua

*DOPS and POPS bilayers.* Starting structures for CHARMM36-UA DOPS and POPS simulations were taken from those generated for the CHARMM36 simulations (see above), with any extraneous hydrogen atoms removed in the lipid tails. Force field parameters for DOPS and POPS were constructed through a combination of the published CHARMM36 PS<sup>3</sup> and CHARMM36-UA PC parameters.<sup>40</sup> All other simulation parameters and conditions were identical to those described for the CHARMM36 all-atom DOPS and POPS simulations.

## S1.3 MacRog

*POPC bilayers.* The POPC bilayer consisting of a total of 128 lipids was constructed from single lipid structure taken from Ref. 41. The bilayer was hydrated by a total of 5120 water molecules, corresponding to 40 water molecules per lipid. The MacRog lipid parameters,<sup>42</sup> obtained from Ref. 41, were used, along with the TIP3P water model.<sup>43</sup> The simulation parameters were identical to those used for POPC/POPC mixtures with the MacRog force field, see below. The simulation was run for 200 ns using Gromacs 2016.3,<sup>30</sup> out of which 150 ns were used for analyses. The simulation data and related files are available from Ref. 44.

*POPS bilayers with Na<sup>+</sup> counterions.* Force field parameters for POPS simulations with the MacRog OPLS-AA force field<sup>11,42,45</sup> were constructed manually using the provided PS parameters as a guide.<sup>45</sup> The original parameters were not used due to an incorrect arrangement of the *sn*-1 and *sn*-2 tails (i.e. the lipid was OPPS and not POPS). The corrected parameters are available from Ref. 46. The starting structure was the same as that used in the CHARMM36 POPS simulations (with Na<sup>+</sup> ions) and was converted into the correct format using a script to adjust the atom order. Water was treated using the TIP3P

model.<sup>43</sup> Simulation parameters were chosen to closely mimic those used in the original force field publications:<sup>11,42,45</sup> van der Waals interactions were truncated at 1.0 nm with a dispersion correction applied to the energy and pressure; Long-range Coulombic interactions were treated with PME beyond a system-optimized cut-off. All other simulation settings were identical to those described above for the CHARMM36 DOPS and POPS simulations, including use of the Verlet cut-off scheme,<sup>47</sup> apart from the use of LINCS to constrain all bonds during these simulations. Simulations with the group cut-off scheme gave slightly lower area per molecule ( $\sim 50\text{\AA}^2$ ) than the simulations with Verlet cut-off ( $\sim 52\text{\AA}^2$ ).

*POPS bilayers with K<sup>+</sup> counterions.* The membrane with sodium counterions was further simulated after replacing Na<sup>+</sup> counterions by K<sup>+</sup> ones, which were described by the Åqvist parameters.<sup>48</sup> Other topologies were unchanged. The simulation parameters were the same as used for the POPC/POPS mixtures with the MacRog force field, see below. The simulation was run for 200 ns, out of which 150 ns was used in the analyses.

#### *POPC:POPS (5:1) mixtures with additional potassium ions*

The bilayers containing a total of 120 POPC and 24 POPS molecules distributed evenly among the two leaflets were set up using CHARMM-GUI.<sup>26,27</sup> The bilayers were solvated by 5760 water molecules, corresponding to 40 water molecules for lipid. Additionally, 24 potassium ions were added to neutralize the charge of the POPS head groups. These bilayers were simulated using Gromacs 2016.3<sup>30</sup> in the presence of counterions only, as well as together with different concentrations of CaCl<sub>2</sub> or KCl. For the former, concentrations of 100 mM, 300 mM, 1 M, and 3 M were considered, which corresponded to the amounts of 10/20, 31/62, 104/208, and 311/622 of Ca<sup>2+</sup>/Cl<sup>-</sup> ions. For membranes with KCl, concentrations of 500 mM, 1 M, 2 M, and 3 M were considered, corresponding to 52, 104, 208, or 311 pairs of K<sup>+</sup> and Cl<sup>-</sup> ions.

The lipids were described using the MacRog model.<sup>11,42,45</sup> The POPC topologies were obtained from Ref. 41, whereas the POPS topology was adapted from OPPS topology in Ref. 45 by reversing the order of acyl chains. The initial structures from CHARMM-GUI

were used because they have the naturally occurring L stereoisomer in the POPS head group, instead of the the D stereoisomer present in Ref. 45. TIP3P model<sup>43</sup> was used for water, and the Åqvist parameters,<sup>48</sup> standard for the OPLS force field, were employed for the ions.

The simulation parameters were taken from Ref. 45. Periodic boundary conditions were employed in all dimensions. The list of neighbors was updated every step. The Lennard-Jones interactions were cut off at 1 nm, whereas the smooth particle mesh Ewald algorithm<sup>37</sup> was used for long-range electrostatics. Dispersion correction<sup>49</sup> was applied to both energy and pressure. Temperature was kept constant at 298 K using the Nosé–Hoover thermostat.<sup>33,34</sup> The lipids and the solvent were coupled separately, and a time constant of 0.4 ps was employed. Pressure was maintained semi-isotropically at 1 bar using the Parrinello–Rahman barostat with a time constant of 1 ps.<sup>35</sup> All non-water bonds were constrained with the LINCS algorithm,<sup>31,32</sup> whereas the bonds in water molecules were constrained using SETTLE.<sup>50</sup> The integration time step was set to 2 fs, and the simulations were performed either for 400 ns (only counterions), 300 ns (systems with KCl), or 600 ns (systems with CaCl<sub>2</sub>). The last 250, 200, or 300 ns of the simulations were included in the analyses, respectively.

## S1.4 Lipid17

*DOPS and POPS bilayers.* The structure of the bilayers with 128 DOPS or 128 POPS lipids were obtained from CHARMM-GUI.<sup>26,27</sup> Bilayers are solvated with 4480 water molecules resulting in 31.1 water molecules per lipid. For each system, 128 NaCl molecules are added to neutralize the system. In all simulations, TIP3P<sup>51</sup> was used as the solvent. SETTLE<sup>50</sup> algorithm was employed to constrain the bonds in TIP3P water molecules. Simulations were ran using Amber18 simulation package<sup>52</sup> and lipid parameters were obtained from Amber Lipid17 force field.<sup>15</sup> For the ions, one set of simulations were run with Joung–Cheatham ion parameters<sup>53</sup> and one set of simulations were run with ff99SB (Åqvist)<sup>48</sup> ion parameters. The data in Table 1 and Refs 54–57 contain the number of molecules in simulations, related simulation files and trajectories.

Each bilayer structure was first minimized for 2500 steps with steepest descent and an additional 2500 step with the conjugate gradient algorithms while restraining the solvent and ion molecules with a force constant  $500 \text{ kcal mol}^{-1} \text{ \AA}^{-2}$ . An additional minimization step was used with the same parameters after removing the constraints on the solvent and ion molecules. During the minimization procedure, non-periodic boundary conditions were applied, no pressure scaling was used and none of the bonds were restrained. A three step heating procedure was applied: in the first heating step the system temperature is increased from 0.0 K to 100.0 K using Langevin thermostat with  $5.0 \text{ ps}^{-1}$  collision frequency while restraining the lipid positions with harmonic springs of force constant  $20.0 \text{ kcal mol}^{-1} \text{ \AA}^{-1}$  at constant volume without periodic boundary conditions. In the second heating step, the system temperature was increased from 100.0 K to 200.0 K using Langevin thermostat with  $5.0 \text{ ps}^{-1}$  collision frequency within 10000 steps while restraining the lipid positions with harmonic springs of force constant  $10.0 \text{ kcal mol}^{-1} \text{ \AA}^{-1}$  at constant volume. In the third heating step, the system temperature is increased from 200.0 K to 303.0 K within 10000 steps using Langevin thermostat with  $5.0 \text{ ps}^{-1}$  collision frequency while restraining the lipid positions with harmonic springs of force constant  $10.0 \text{ kcal mol}^{-1} \text{ \AA}^{-1}$  at 1 bar constant pressure using Berendsen barostat with 3.0 ps relaxation time. From the second heating step onward, periodic boundary conditions in all dimensions were applied. The semi-isotropic pressure coupling along  $xy$ -plane was employed and the surface tension was set to 0.0 dyn explicitly. After the third heating step, each structure is equilibrated for 100 ns at 1 bar and 303 K constant pressure using Berendsen barostat and temperature using Langevin thermostat, respectively. For the equilibration step, semi-isotropic pressure coupling along  $xy$ -plane was employed and the surface tension was set to 0.0 dyn explicitly. For all heating and equilibration steps, the lengths of the hydrogen containing bonds were restrained using SHAKE algorithm and a time step of 2 fs was used. In all steps with periodic boundary conditions, the non-bonded interactions are calculated with particle mesh Ewald<sup>37</sup> using 1.0 nm cutoff.

For the production runs, the temperature and pressure were set to 303 K and 1 bar, using Langevin thermostat with  $1.0 \text{ ps}^{-1}$  collision frequency and Berendsen barostat with 1.0 ps relaxation time, respectively. Periodic boundary conditions were applied in all dimensions and the non-bonded interactions are calculated with particle mesh Ewald<sup>37</sup> using 1.0 nm cutoff. The lengths of the hydrogen containing bonds were constrained using SHAKE algorithm and a time step of 2 fs was used. Trajectories are saved in every 10 ps intervals. Two independent trajectories of 500 ns long was generated and the last 200 ns portions were used for the analysis.

*POPC:POPS (5:1) mixtures with additional potassium and sodium ions* The initial structure of the bilayers with 120 POPC and 24 POPS lipids were obtained from CHARMM-GUI.<sup>26,27</sup> Bilayers were solvated with 5760 TIP3P water molecules.<sup>51</sup> For the simulations of the lipids and ions, the Amber Lipid 17<sup>15</sup> and ff99SB<sup>48</sup> force fields were used, respectively. Simulations were ran using Amber18 simulation package<sup>52</sup> The simulation steps are the same as the the simulations of DOPS and POPS bilayers described above, with the only difference that the total simulation time was 300 ns, of which last 200 ns was used for the analysis. The number of ions in each specific system is given in Table S1. The trajectory files can be found in Refs 16–19.

*POPC:POPS (5:1) mixtures with additional calcium chloride concentration with default Amber parameters* Simulations were performed using Amber18 simulation package<sup>52</sup> with ff99SB<sup>48</sup> ion parameters and Amber Lipid17<sup>15</sup> force field. Number of ions and water molecules for this set of simulations are shown in Table 2. The simulation details, minimization, heating, and equilibration runs are the same as described above for the other POPC:POPS (5:1) simulations with Amber Lipid17 forcefield. For each ion concentration, 100 ns equilibration runs were followed by 300 ns production runs with two independent trajectories, of which last 200 ns were used for the analysis. The trajectory files can be found from Ref 58.

*POPC:POPS (5:1) mixtures with additional calcium chloride concentration with Dang ion parameters* The Lipid17 parameters for POPS were obtained from AmberTools18<sup>52</sup> and

converted to Gromacs format using acpype.<sup>59</sup> The previously generated<sup>24</sup> Lipid14 parameters for POPC in Gromacs format were downloaded from Ref. 60. Dang parameters for ions<sup>61,62</sup> were used. Initial structures were generated using CHARMM-GUI<sup>26,27</sup> and simulations were performed using the GROMACS 2018 simulation package<sup>30</sup> with the time step of 2 fs. The non-bonded interactions were calculated directly within 1.0 nm cutoff using the Verlet scheme,<sup>47</sup> and the long-range electrostatic forces were calculated using particle mesh Ewald.<sup>37</sup> The bond lengths of hydrogen atoms were constrained using LINCS algorithm.<sup>31</sup> Temperature was coupled to the velocity rescaling thermostat<sup>63</sup> at 298 K with a coupling constant of 1 ps. Pressure was coupled to the Parrinello–Rahman barostat<sup>35</sup> at 1 bar with a coupling constant of 10 ps. The compositions of individual simulations are shown in Table 2. The systems were equilibrated 50 ns prior to production simulations used for analysis, which are available in Ref. 64 including the simulation settings. Topologies in a format for the GROMACS package are available in the repository 65.

## S1.5 Slipids

*POPS and DOPS with 128 lipids* Starting structures for the Slipids POPS and DOPS (with 128 lipids) simulations were the same as constructed for the CHARMM36 simulations. Force field parameters were taken from the published Slipids PS model,<sup>66</sup> however simulation cut-offs used herein were different to these previously published simulations.<sup>67</sup> This was due to the use of the older GROMACS group-based cut-off scheme in these previous simulations. In the simulations reported in this work, the Verlet cut-off scheme was used. Van der Waals interactions were truncated at 1.0 nm with LJ-PME<sup>68</sup> applied to account for the long-range interactions. Coulombic interactions were truncated at 1.0 nm with PME used for the long-range interactions. Full testing and validation of these settings with the Slipids PS force field will be provided in an additional forthcoming work. All other simulation settings were identical to those described above for the CHARMM36 DOPS and POPS simulations.

*DOPS with 288 lipids.* The starting structure with 288 DOPS lipids, 11232 water molecules

and 288 Na<sup>+</sup> ions was constructed with the MEMBRANE BUILDER website.<sup>69</sup> The Slipids<sup>66</sup> forcefield was used for DOPS, the TIP3P<sup>43</sup> water model was used to solvate the system and ions are described by the parameters derived by Åqvist.<sup>48</sup> The system was simulated in NPT ensemble for 200 ns using the GROMACS 5.0.4 package,<sup>30</sup> and the last 100 ns was used for the analysis. Timestep of 2 fs was used with the leapfrog integrator. The Nosé–Hoover thermostat<sup>33,34</sup> was used with reference temperature of 303 K and a relaxation time constant of 0.5 ps; lipids and water plus ions were coupled separately to the heat bath. Pressure was kept constant at 1.013 bar using a semi-isotropic Parrinello–Rahman barostat<sup>35</sup> with a time constant of 10.0 ps. Long-range electrostatic interactions were calculated using the PME method.<sup>36,37</sup> A real space cut-off of 1.0 nm was employed with grid spacing of 0.12 nm in the reciprocal space. Lennard-Jones potentials were cut off at 1.4 nm, with a dispersion correction applied to both energy and pressure. All covalent bonds in lipids were constrained using the LINCS algorithm,<sup>31</sup> whereas water molecules were constrained using SETTLE.<sup>50</sup> Twin-range cutoffs, 1.0 nm and 1.6 nm, were used for the neighbor lists with the long-range neighbor list updated every 10 steps.

## S1.6 Berger

*POPC bilayers.* Previously published simulation<sup>70</sup> available from Ref. 71 was used for POPC at 310 K.

*DOPS and POPS bilayers.* Starting structures for DOPS and POPS simulations performed with a Berger-based PS force field were taken from those produced for the CHARMM36 simulations. A script was used to re-order the atoms and to remove any extraneous hydrogen atoms. Force field parameters were taken from those published by Mukhopadhyay et al.<sup>21</sup> and the SPC water model was used.<sup>72</sup> The simulation cut-offs closely matched those of Mukhopadhyay et al.: van der Waals interactions were truncated at 1.0 nm; Coulombic interactions were truncated at 1.0 nm with PME applied to account for the interactions beyond the cut-off. All other simulation settings were identical to those described above

for the CHARMM36 DOPS and POPS simulations, including the use of the Verlet cut-off scheme, apart from all bonds were constrained using LINCS in these simulations.

*POPC:POPS (4:1) mixtures with additional sodium and calcium ions.* Previously published simulations with the additional amount of sodium<sup>73</sup> available from Ref. 23 and with the additional amounts of calcium<sup>74</sup> available from Refs. 75,76 were used. To generate the reference system with sodium counterions only, the additional ions were removed from the structure file in Ref. 23. This system was simulated 120 ns using Gromacs 5<sup>30</sup> with parameter (mdp file) and force field files (top and itp) available from Ref. 22, the last 80 ns was used for the analysis.

## S1.7 GROMOS-CKP and GROMOS-CKPM

The GROMOS-CKP force field (CKP stands for Chandrasekhar-Kukol-Piggot) contains a set of GROMOS compatible lipid parameters. Parameters have been developed and validated for PC,<sup>77-79</sup> PE, PG, Cardiolipin<sup>80</sup> and PI<sup>81</sup> lipids, amongst others. Within this work we provide an initial validation for simulating PS lipids with two variants of this force field (termed GROMOS-CKP and GROMOS-CKPM). Additional forthcoming work will provide additional validation and testing of these PS parameters. The two variants of the force field only differ in terms of the charges in the head group. The GROMOS-CKPM (M stands for Mukhopadhyay after the first published Berger-based PS simulations published; see above for further details) lipid uses Berger/Chiu based charges for the NH3 part of the PS head group (i.e. has the same charges as used in the choline part of the Berger PC lipids). The GROMOS-CKP parameters use charges compatible with the rest of the GROMOS force fields; the charges of the NH3 part of the PS head group were taken from a lysine side-chain of the GROMOS 54A7 protein force field<sup>82</sup> The remainder of the parameters were assigned by analogy from either the other GROMOS-CKP lipids or the GROMOS 54A7 force field. *DOPS and POPS bilayers.* Starting structures for GROMOS-CKP and GROMOS-CKPM simulations were taken from those produced for the CHARMM36 simulations. A script was

used to re-order the atoms and to remove any extraneous hydrogen atoms. The force fields parameters for DOPS and POPS were as discussed above. The SPC water model was used in these simulations.<sup>72</sup> Simulation cut-offs were chosen to closely match those used in the original GROMOS-CKP force field validation: van der Waals interactions were truncated at 1.4 nm with a dispersion correction applied to the energy and pressure; Coulombic interactions were also truncated at 1.4 nm with PME used to treat the long-range interactions. All other simulation settings were identical to those described above for the CHARMM36 DOPS and POPS simulations, including the use of the Verlet cut-off scheme, apart from all bonds were constrained using LINCS in these simulations.

*POPC:POPS (5:1) mixtures without additional ions* Starting structures for GROMOS-CKP and GROMOS-CKPM simulations were taken from those produced for the equivalent CHARMM36 simulations (see above). A script was used to re-order the atoms and to remove any extraneous hydrogen atoms. Simulation setting were identical to those as described above for the GROMOS-CKP(M) POPS bilayers.

## S2 Electrometer concept in PC lipid bilayers mixed with negatively charged lipids

The electrometer concept is based on the empirical observations that the order parameters of  $\alpha$  and  $\beta$  carbons in PC lipid headgroup decrease (increase) proportionally to the bound positive (negative) charge<sup>83–86</sup> (Fig. S1). Therefore, the headgroup order parameters can be used to measure the ion binding affinity to lipid bilayers containing PC lipids.<sup>1,83–85,87,88</sup> Changes of the headgroup order parameters of negatively charged PS and PG lipids are also systematic, but less well characterized.<sup>1,87–89</sup> Therefore, the ion binding affinity to negatively charged bilayers can be better characterized measuring the PC headgroup order parameters from mixed bilayers.<sup>1,87–90</sup>

When using the PC headgroup order parameters to evaluate the ion binding affinity to a

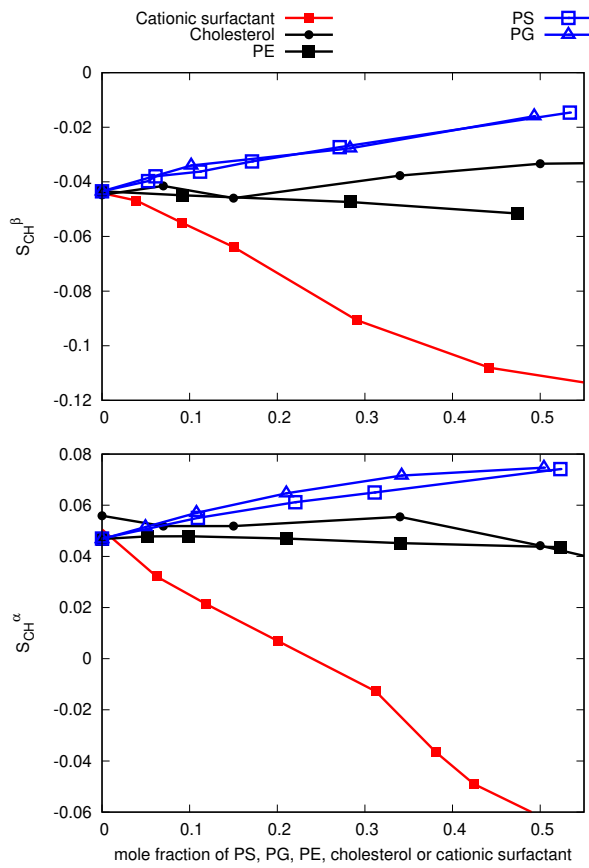


Figure S1: Headgroup order parameters of POPC measured from mixtures with PS (bovine brain), POPG, POPE, cholesterol and cationic dihexadecyldimethylammonium bromide (DHAB) surfactant.<sup>86,91,92</sup> Signs are taken from separate experiments.<sup>93,94</sup>

bilayer containing anionic lipids, it is important to note that the order parameters increase due to the addition of negative charged lipids according to the electrometer concept<sup>85,91</sup> (Fig. S1). Therefore, the PC headgroup order parameters are larger in mixtures with anionic lipids than in pure lipid bilayers. This is evident also in the headgroup order parameters of POPC in bilayers with different amounts anionic lipids without added calcium (Fig. S2). Upon addition of  $\text{CaCl}_2$ , the order parameters decrease and reach the values of pure PC bilayer close to the  $\text{CaCl}_2$  concentrations of  $\sim 50\text{--}300\text{mM}$ , depending on the amount of negatively charged lipids in the mixture (Fig. S2). Around these concentrations the positive charge of bound  $\text{Ca}^{2+}$  cancels the negative charge lipids, resulting to a neutral membrane. Above such concentrations, the specific binding of calcium leads to the overcharging of the membrane.

Because the POPC headgroup order parameters in mixtures with different amounts of anionic lipids but without additional salt are not equal, the binding affinity of calcium can be better compared by plotting the changes of order parameters as a function of added calcium. As expected, such a plot reveals more pronounced order parameter decrease in systems with larger fractions of negatively charged lipids (Fig. S3), indicating an increase in the calcium binding affinity with the increasing amount of negatively charged lipids in membranes. In conclusion, the presented empirical comparison of headgroup order parameter changes from various mixtures of POPC and anionic lipids with added calcium gives physically consistent results, suggesting that the electrometer concept can be used to determine the cation binding affinity also to the lipid bilayers containing mixtures of PC and anionic lipids.

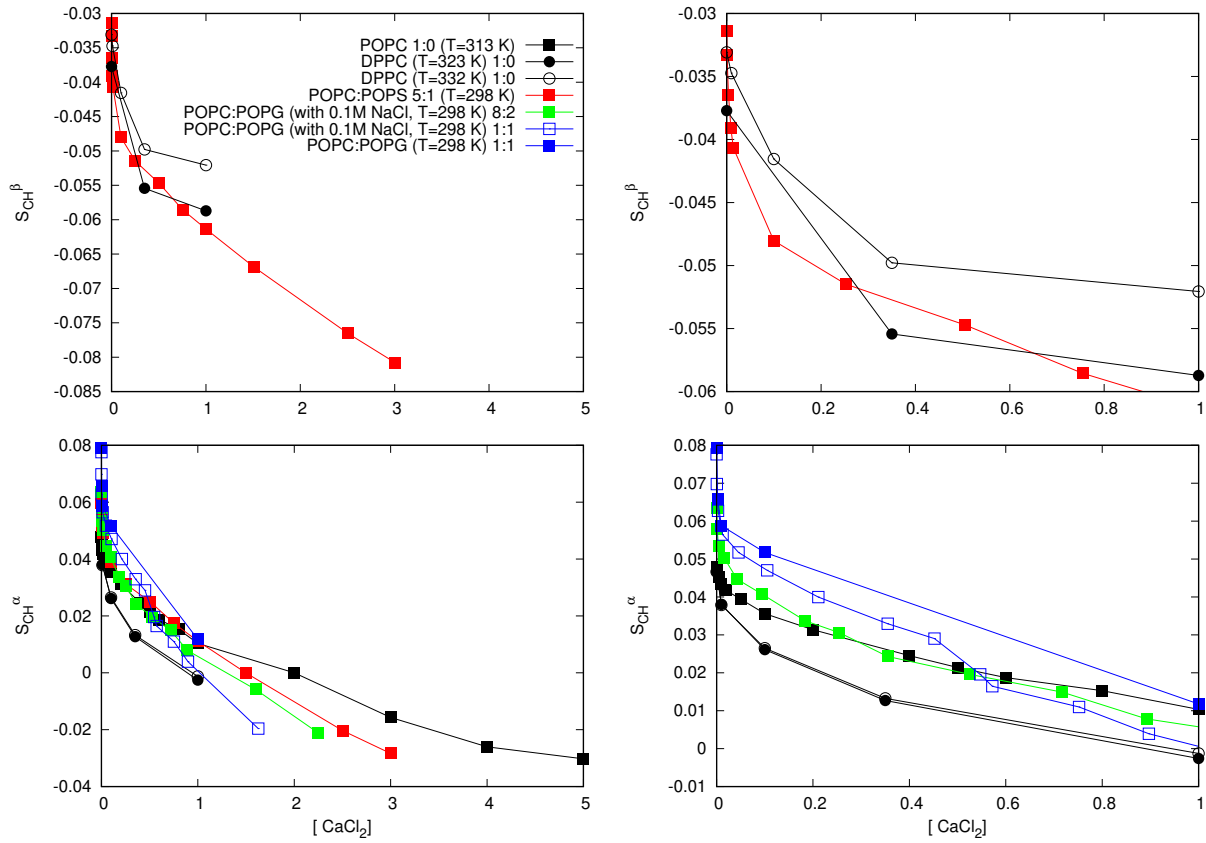


Figure S2: Headgroup order parameters of POPC as a function of  $\text{CaCl}_2$  concentration from experiments with different mole fractions of negatively charged lipids (left column). Right column shows the same data zoomed to the concentrations below 1 M. Data for Pure DPPC from Ref. 83, for pure POPC from Ref. 84, for POPC:POPS (5:1) mixture from Ref. 1, for POPC:POPG (8:2,1:1) mixtures with 0.1 M NaCl from Ref. 88 and for POPC:POPG (1:1) mixture data without NaCl from Ref. 87.

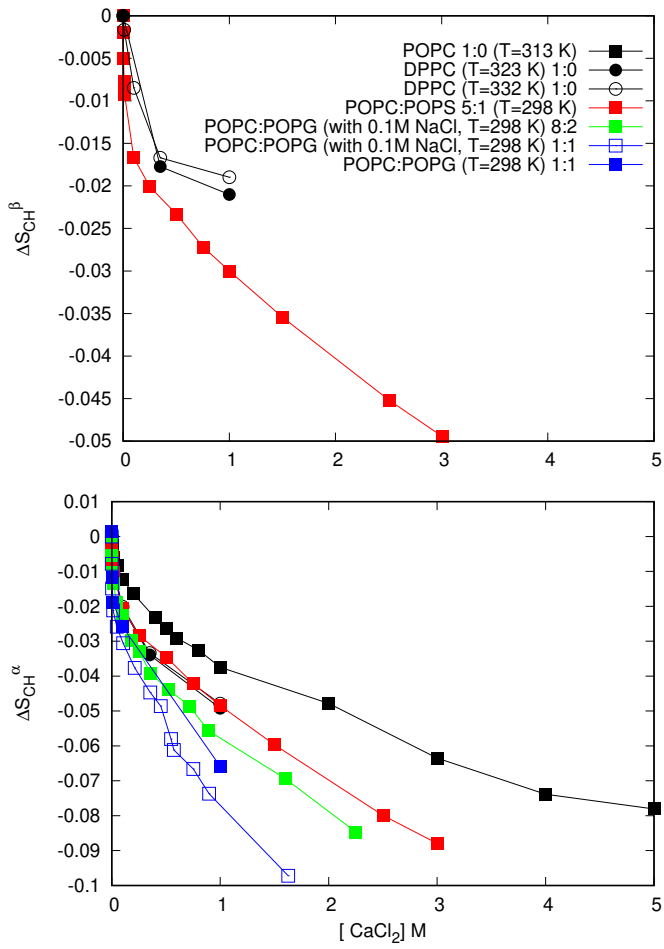


Figure S3: Changes of POPC headgroup order parameters as a function of  $\text{CaCl}_2$  measured from mixed bilayers containing different amounts of anionic lipids. The original data is the same as in figure S2.

### S3 Calibration of PC headgroup order parameter response to the bound cations

When using the molecular electrometer concept to compare ion binding affinity between simulations and experiments, one needs to keep in mind that two things affect how much a given order parameter changes when solution charge content is varied: 1) the change in the amount of bound charge and 2) the sensitivity of the order parameter to bound charge. Therefore, the response of the order parameters to the bound charge in simulations needs to be first calibrated against experiments.<sup>95,96</sup>

In our previous work,<sup>95</sup> we investigated the change in order parameters under varying concentrations of mono- and divalent salts and concluded that the experimental  $\Delta S_{\text{CH}}^{\beta}/\Delta S_{\text{CH}}^{\alpha}$  ratio<sup>83</sup> was well reproduced by the Lipid14 model, but underestimated by other force fields. In a more recent study,<sup>96</sup> the headgroup order parameter responses were compared more carefully with the experiments of cationic dihexadecyldimethylammonium bromide (DHAB) surfactants in POPC bilayer.<sup>86</sup> The advantage of this approach is that the amount of DHAB in the bilayer is exactly known in experiments, which can be exploited to extract the sensitivity of the order parameters. This revealed that both  $S_{\text{CH}}^{\beta}$  and  $S_{\text{CH}}^{\alpha}$  in the Lipid14 model are equally oversensitive (and thus giving the correct  $\Delta S_{\text{CH}}^{\beta}/\Delta S_{\text{CH}}^{\alpha}$ ) to the bound charge, whereas CHARMM36 gives better agreement for the  $\alpha$  carbon (Fig. S4), indicating that the headgroup order parameter response to the bound charge is actually more realistic in CHARMM36 compared to Lipid14. The ratio was overestimated for the CHARMM36 model because the  $\beta$ -carbon order parameter is relatively more sensitive than the  $\alpha$ -carbon order parameter.

That being said, in the force fields investigated so far, the discrepancies arising from the sensitivity of lipid headgroup to bound charge are typically smaller than the discrepancies arising from ion binding affinity.

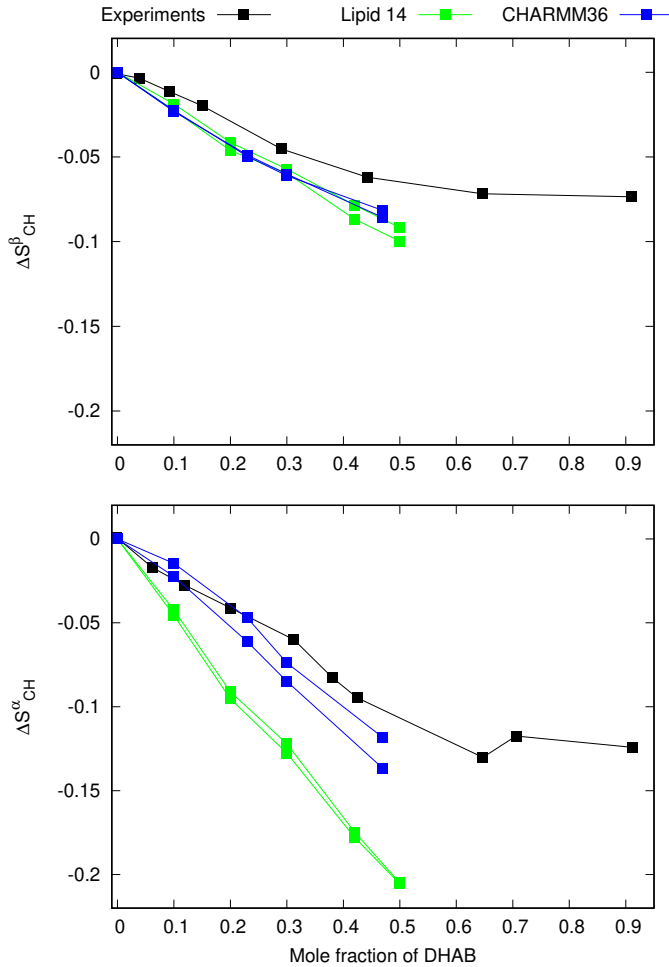


Figure S4: Responses of headgroup order parameters to the fixed amount of cationic surfactants in POPC bilayer from simulations and experiments.<sup>86</sup> The simulation results for Lipid14 are directly from Ref. 96. The CHARMM36 simulation data and details are available from Ref. 97.

## S4 Sensitivity of the molecular electrometer to the chosen definition of ion concentration

Previous studies using the electrometer concept to assess the ion binding affinity to lipid bilayers report ion concentrations either in water before solvating the lipids (buffer concentration)<sup>1,83,95</sup> or in bulk water after solvating the lipids (bulk concentration).<sup>84,96</sup> In this work, we use the former definition to be consistent with the experimental reference data.<sup>1</sup> The difference between these two concentrations increases with the increasing ion binding affinity. However, Fig. S5 demonstrates that in a model with realistic ion binding affinity<sup>96</sup> the deviation between the two definitions is negligible.

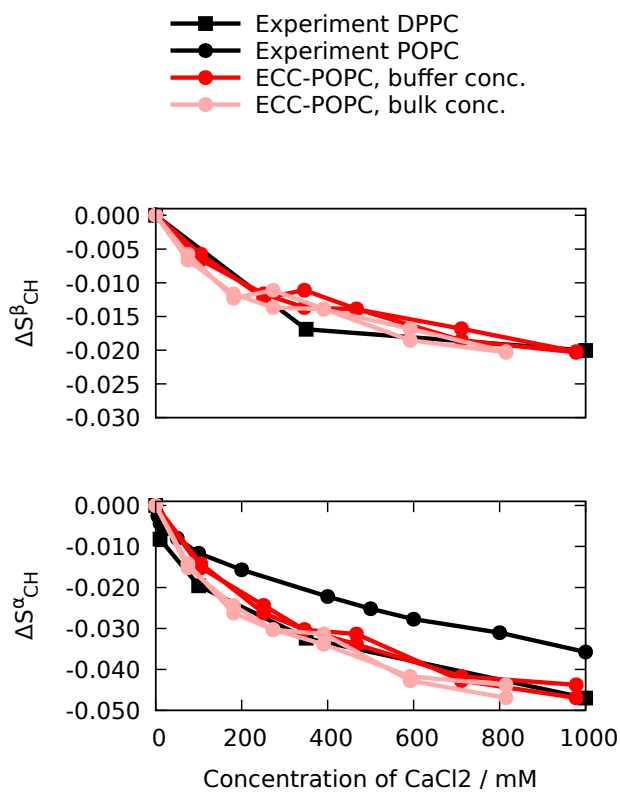


Figure S5: Changes of the headgroup order parameters as a function of  $\text{CaCl}_2$  concentration using two possible definitions of ion concentration from the recent force field with realistic calcium binding affinity to a POPC bilayer<sup>96</sup> together with the experimental data.<sup>83,84</sup>

## S5 Spectral slices in the indirect dimension from the R-PDLF and SDROSS experiments

The C–H bond order parameters of the headgroup and glycerol backbone carbons are determined as  $S_{\text{CH}} = \Delta\nu / (0.315 \times 21.5\text{kHz})$ , where  $\Delta\nu$  is the dipolar splitting given by the largest peak widths observed in the second dimension of the R-PDLF spectra (blue lines in Fig. S6), 0.315 is the scaling factor of the R18 recoupling sequence and 21.5 kHz is the maximum  $^1\text{H}$ – $^{13}\text{C}$  dipolar coupling for a C–H bond.<sup>98</sup> The resulting order parameters are in good agreement with the previously reported values from  $^2\text{H}$  NMR experiments<sup>99</sup> (Fig. 2 in the main text). However, the resolution in our  $^{13}\text{C}$  NMR experiment was not sufficient to detect the the splitting related to the smaller order parameter of the C–H bond in the  $\alpha$  carbon observed in  $^2\text{H}$  NMR experiments.<sup>99</sup> Therefore, the value of  $0 \pm 0.02$  from our  $^{13}\text{C}$  NMR experiments is shown figure 2 and the magnitude of 0.02 from the literature is used in the SIMPSON calculations in the main text.

Interpretation of the order parameter signs of the  $\alpha$  carbon from the SDROSS experiment is complicated by the presence of distinct order parameters for the two attached hydrogens. As discussed in the main text, interpretation of the SDROSS curve with the help of SIMPSON simulations gave values +0.09 and –0.02 for the  $\alpha$ -carbon order parameters. To corroborate our interpretation, we measured the SDROSS curve also using the higher 8 kHz MAS frequency (Fig. S6 bottom), which makes the experiment more sensitive to larger order parameter values. Also this experiment indicates a positive value for the larger  $\alpha$ -carbon order parameter.

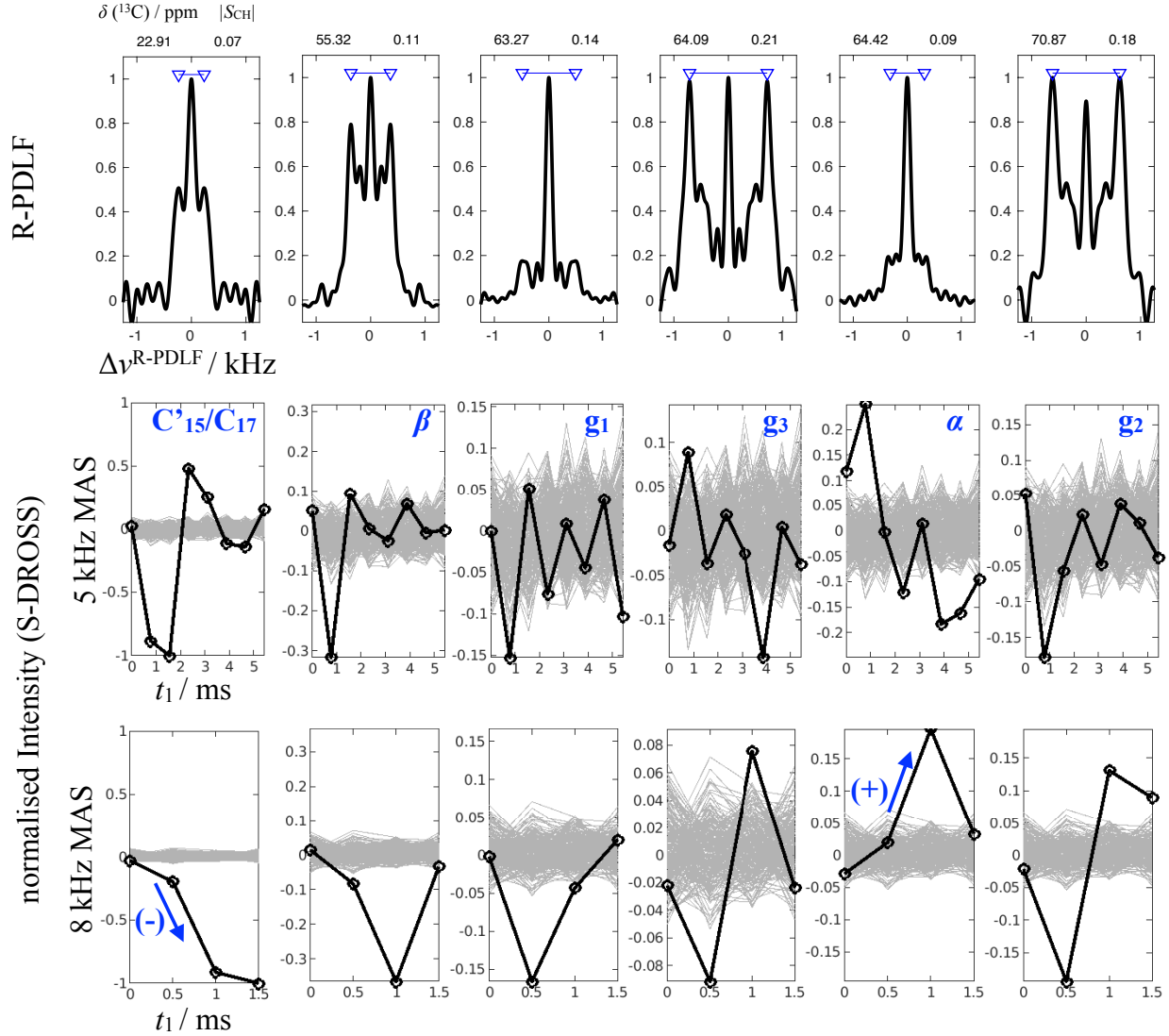


Figure S6: Spectral slices in indirect dimension from the R-PDLF (top) and S-DROSS (middle and bottom) experiments at distinct chemical shifts. The chemical shifts and order parameters (calculated from the dipolar splittings indicated with blue lines in the R-PDLF slices) are shown on top each column (chemical shift left, order parameter right). The assignment of columns is given in the middle. The SDROSS slices were measured using both 5 KHz (middle) and 8 kHz (bottom) because different MAS frequencies enable the higher sensitivity to the order parameters with lower and higher magnitudes, respectively. The background noise taken from chemical shift slices without carbon peaks (grey lines in SDROSS figures) are used to determine the error bars for  $\alpha$  and  $\beta$  carbons in Fig. 1 in the main text. The SDROSS profile of the acyl chain methyl carbons (left column) was used as reference assuming that these carbons have negative order parameters.

## **S6 Dihedral angle distributions of the headgroup and glycerol backbone regions of PS lipids from different simulation models**

The dihedral angles and structures of the glycerol backbone and headgroup regions of POPS lipids show wide variety between different simulation models (Figs. S7, S8 and S9). Detailed discussion of the structural differences is limited by the lack of realistic model that would correctly reproduce the headgroup and glycerol backbone order parameters. However, some structural characteristics of PS headgroup can be suggested based on the best available models (Figs. S10, S11 and S12), as discussed in the main text. The glycerol backbone structures are not discussed in this work because our focus is on PS headgroup. However, the data presented here can be useful for future investigations.

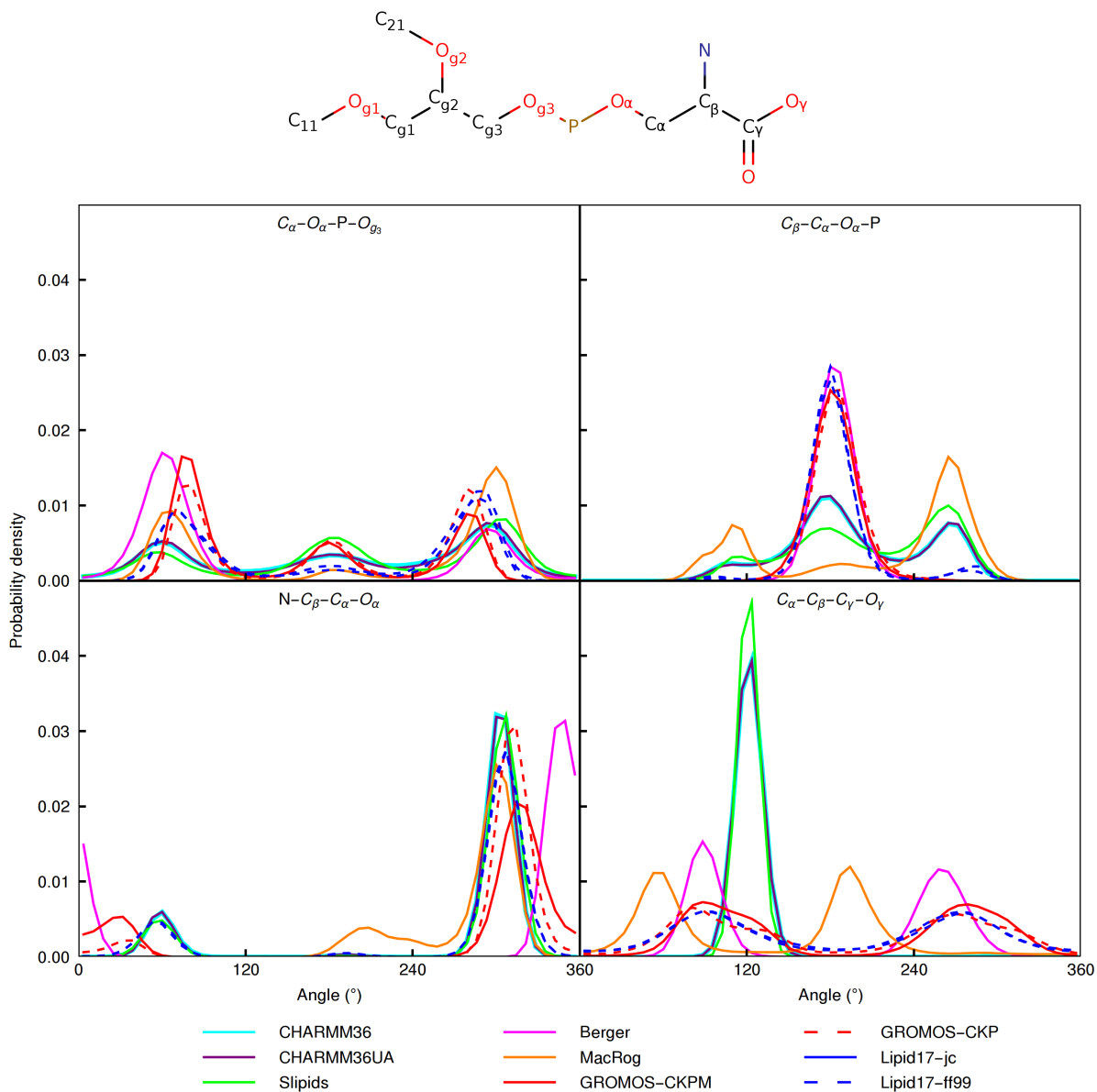


Figure S7: Dihedral angle distributions of the headgroup region of POPS from different simulation models.

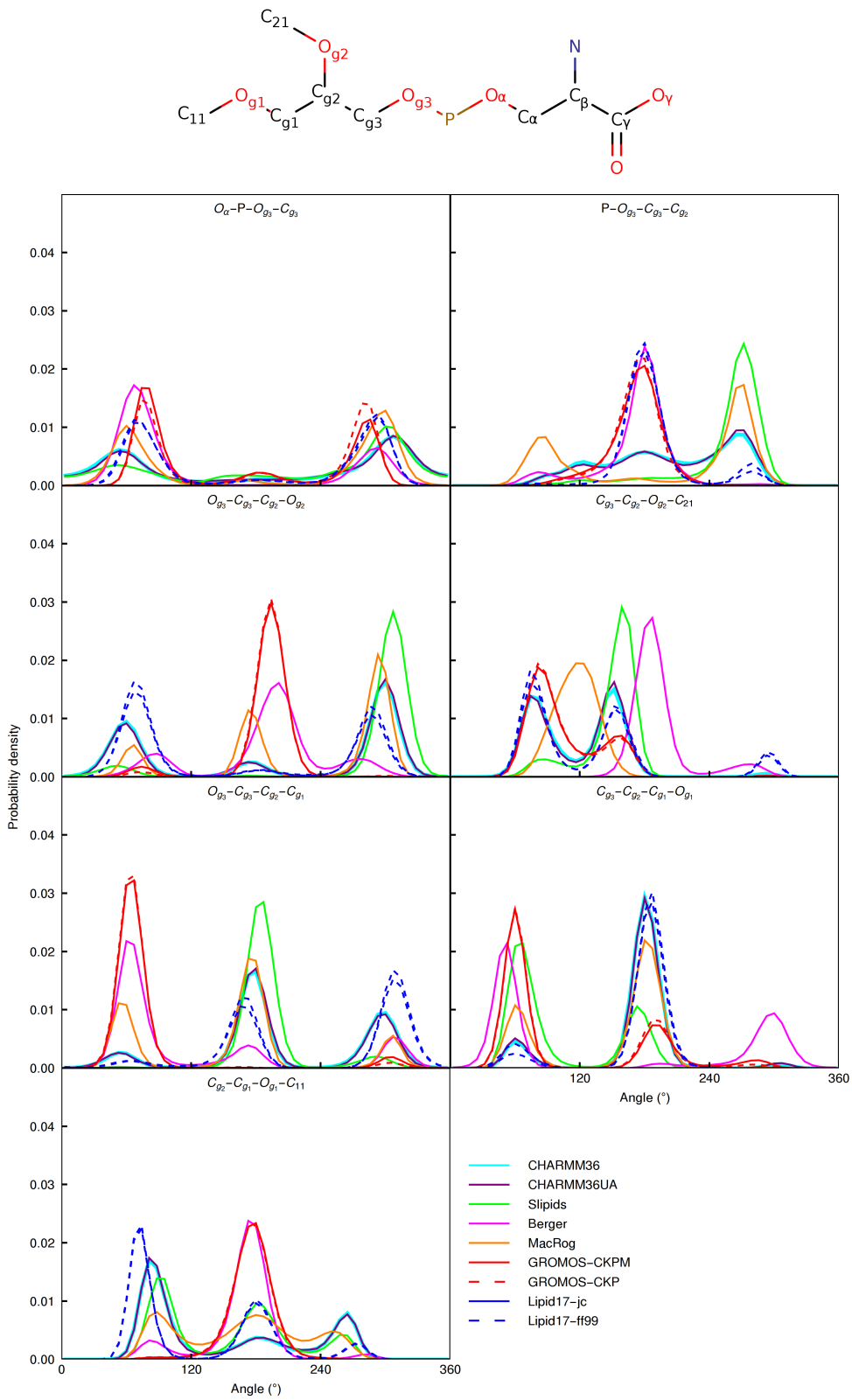


Figure S8: Dihedral angle distributions of the glycerol backbone region of POPS lipids from different simulation models.

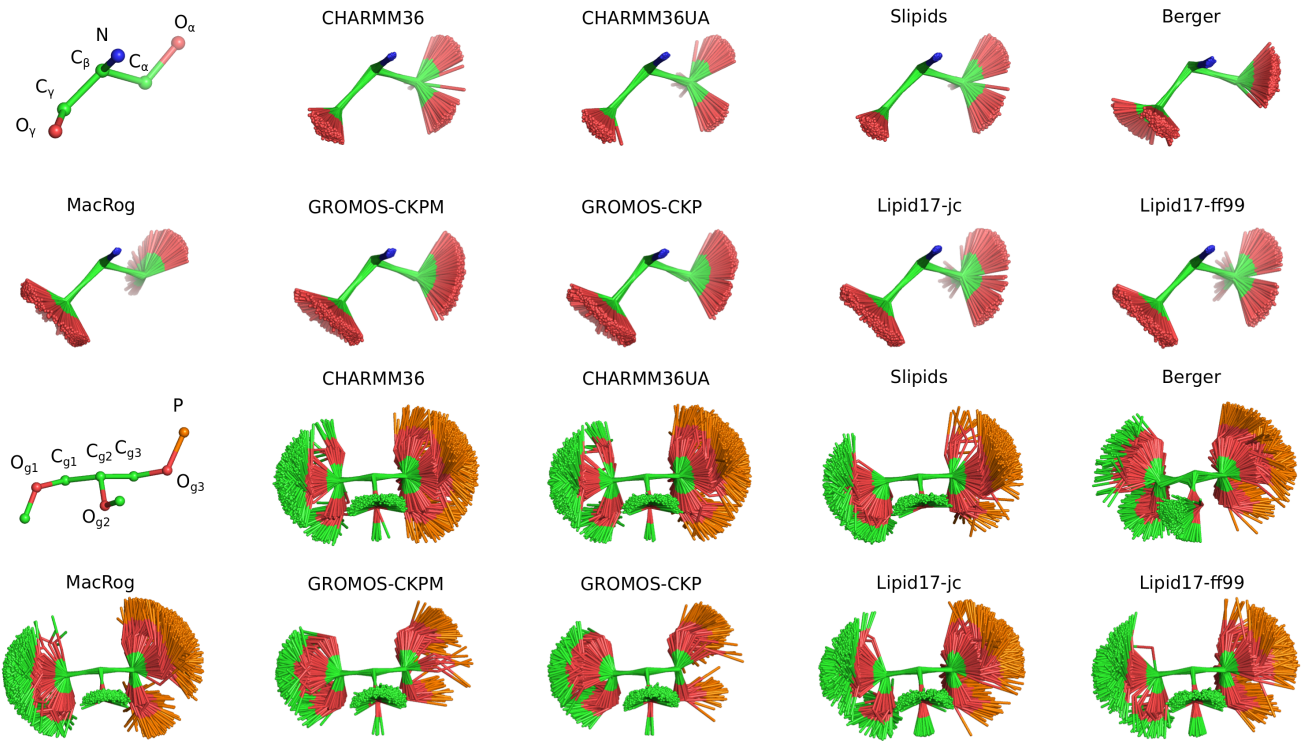


Figure S9: Overlayed snapshots of the headgroup ( $C_{\gamma}$ - $C_{\beta}$ - $C_{\alpha}$  carbons overlayed) and glycerol backbone ( $C_{g1}$ - $C_{g2}$ - $C_{g3}$  carbons overlayed) regions from different POPS simulations. Note that only one of the two  $O_{\gamma}$  atoms in the carboxylate group from PS lipids is shown.

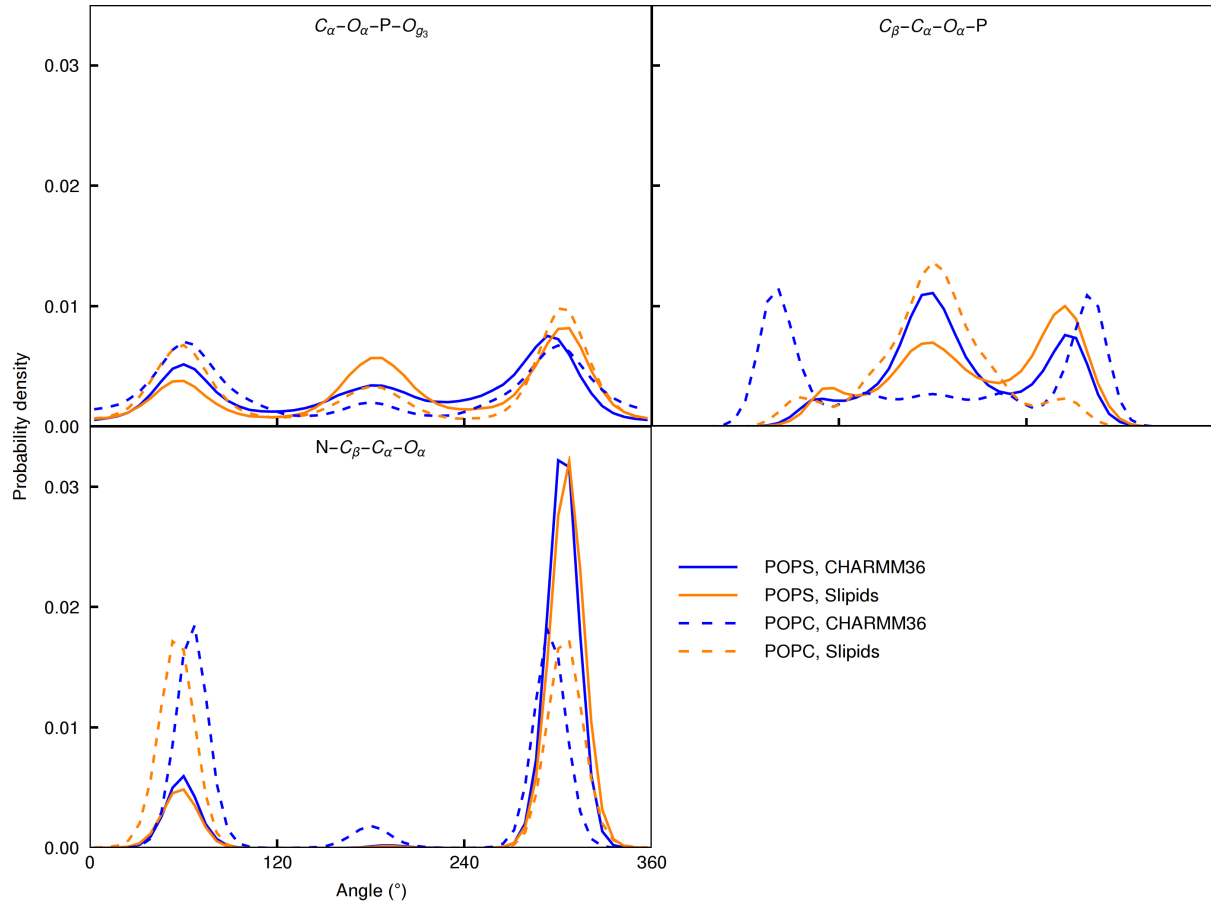


Figure S10: Dihedral angle distributions of the headgroup regions from CHARMM36 and Slipids simulations compared between the POPC and POPS lipids. The CHARMM36 POPC simulation is from Ref. 100 and Slipids POPC from Ref. 101.

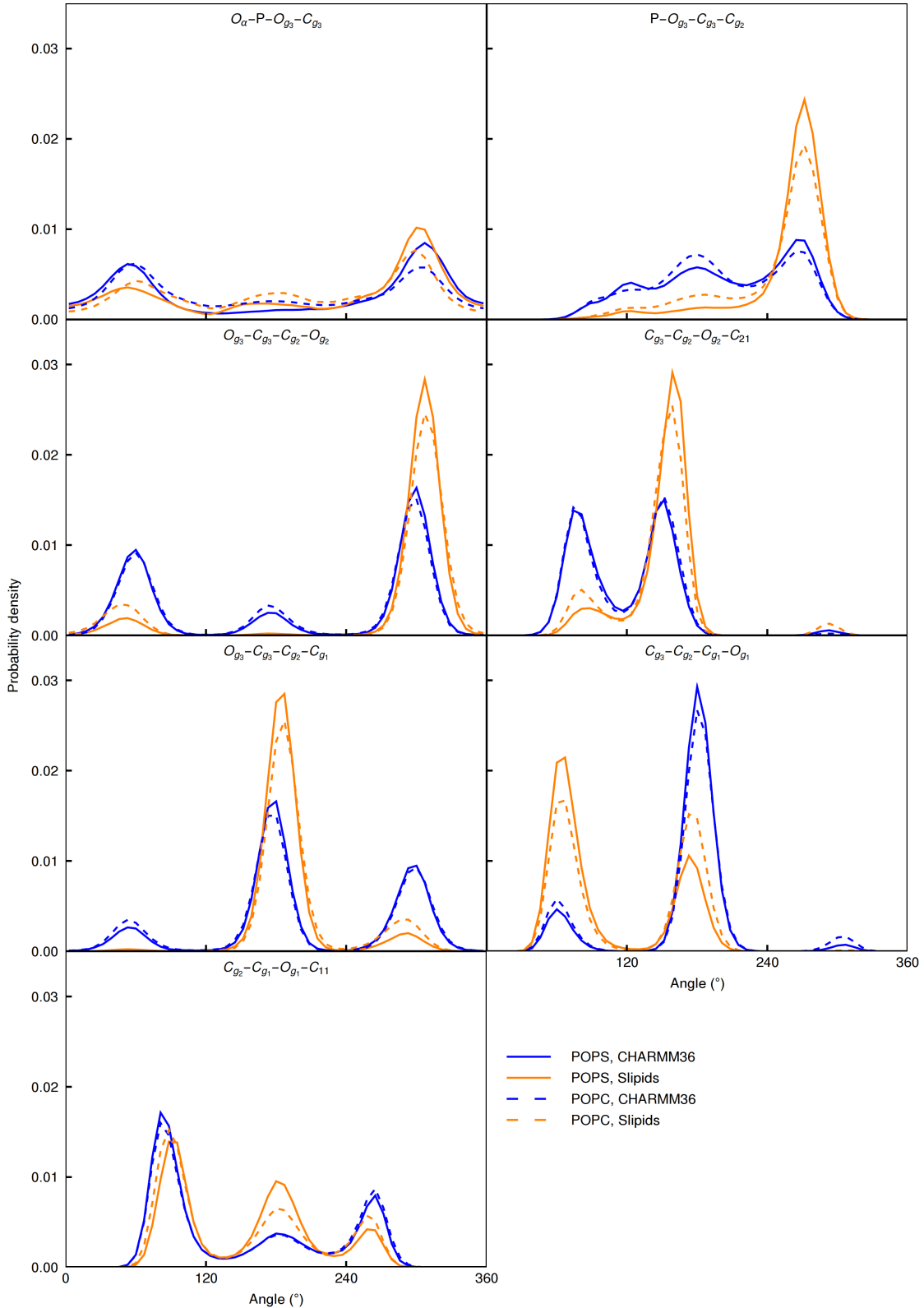


Figure S11: Dihedral angle distributions of the glycerol backbone regions from CHARMM36 and Slipids simulations compared between the POPC and POPS lipids. The CHARMM36 POPC simulation is from Ref. 100 and Slipids POPC from Ref. 101.

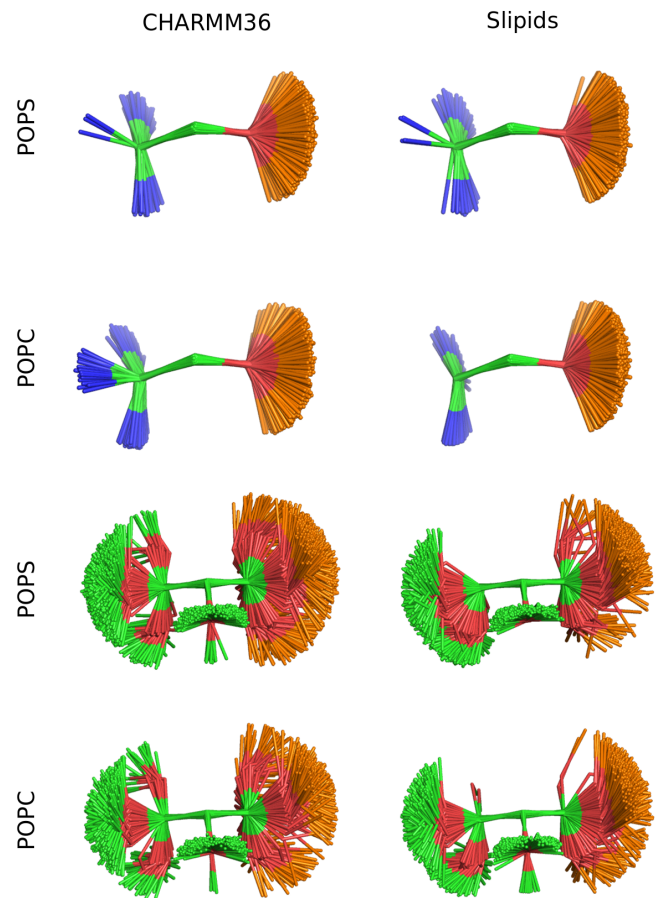


Figure S12: Overlayed snapshots of the headgroup and glycerol backbone regions from CHARMM36 and Slipids simulations compared between the POPC and POPS lipids. The CHARMM36 POPC simulation is from Ref. 100 and Slipids POPC from Ref. 101.

## S7 Headgroup response to the additional counterions in POPC:POPS (5:1) mixtures

To evaluate counterion binding in different simulation models against experimental data,<sup>1</sup> we plot the headgroup order parameters measured from POPC:POPS 5:1 mixture as a function of different monovalent ions added to the buffer (Fig. S13). Experimental order parameters of POPC headgroup in the mixture are available as a function of LiCl and KCl concentrations, while POPS headgroup order parameters are measured also in increasing NaCl concentration. Lithium interacts more strongly with PS headgroups than other monovalent ions,<sup>1,89,102–104</sup> as also observed for PC headgroups.<sup>105</sup> The different binding behaviour is evident based on the response of PS headgroup order parameters, which decrease with the addition of lithium but increase with the addition of sodium or potassium (Fig. S13). POPC headgroup order parameters exhibit a clear decrease as a function of LiCl concentration but only modest changes as a function of KCl concentration, indicating significant Li<sup>+</sup> binding but only weak K<sup>+</sup> binding to the mixture when interpreted using the electrometer concept.<sup>83–85</sup>

In simulations with Berger and CHARMM36 models, the responses of POPC and POPS order parameter to added sodium and potassium are not in line with the experiments. Instead, the simulations produce a response similar to experiments conducted in LiCl (Fig. S13), indicating overestimated binding affinity of sodium and potassium in these simulations. The MacRog simulations with potassium exhibit weaker counterion binding affinity (Fig. S14), but significantly larger error bars and less systematic changes in the order parameters (Fig. S13). Similar unsystematic behaviour was also observed in the simulations of Lipid14/17 model with the additional counterions,<sup>16–19</sup> for which the data is not shown due to the formation of ion clusters in water with relatively low (1 M) ion concentrations (Fig. S15). Appearance of such clusters in the MagRog simulations with 4 M KCl could explain the unsystematic changes of the order parameters in this model upon increasing KCl. In conclusion, the results are in line with the Section in the main text, suggesting that the MacRog simulations with

KCl give the most realistic surface charge at the lipid bilayer interface among the tested simulation models.

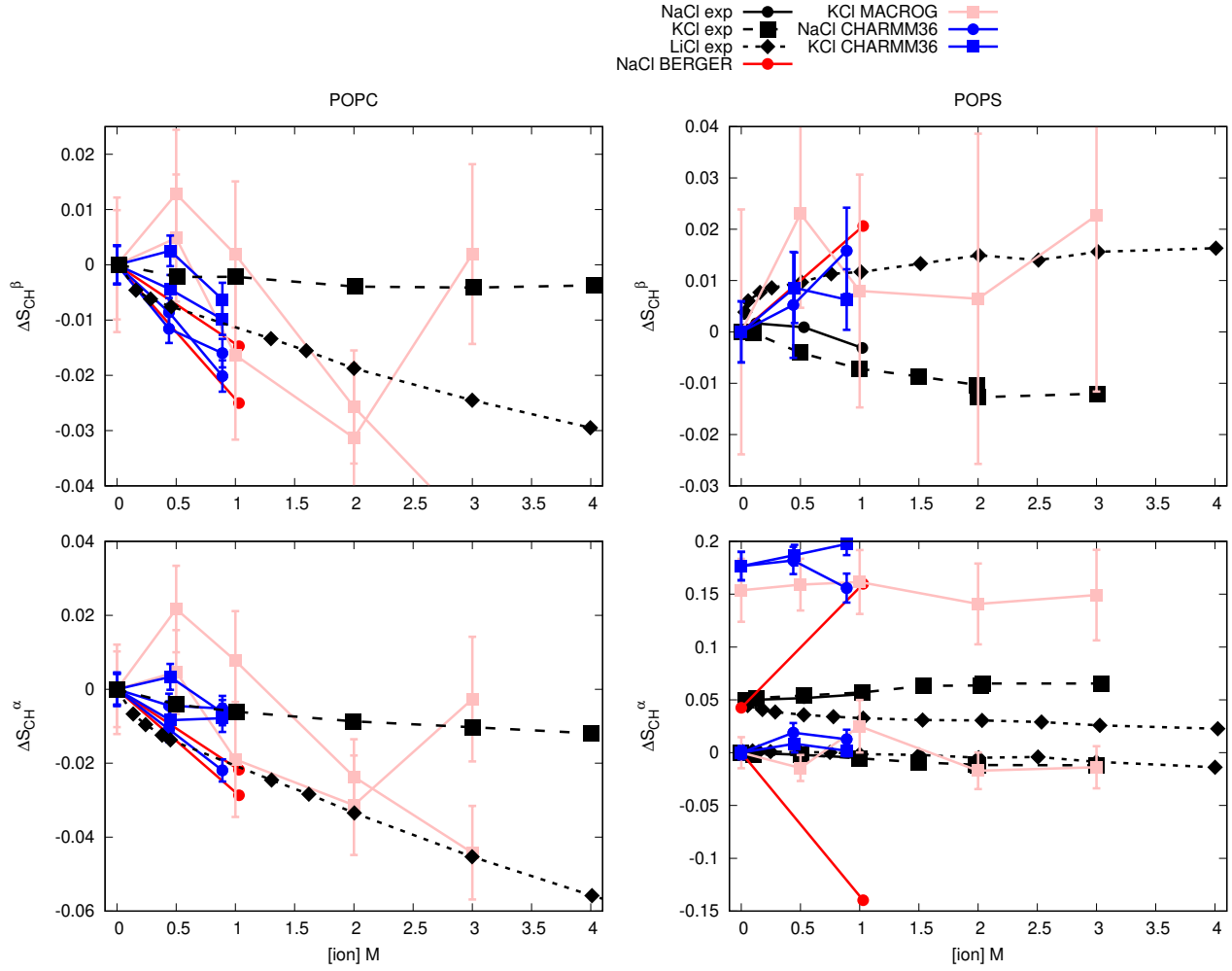


Figure S13: Changes of the PC (left) and PS (right) headgroup order parameters as a function of added NaCl, KCl and LiCl from POPC:POPS (5:1) mixture at 298 K (except Berger simulations are (4:1) mixture at 310 K). The experimental data is from Ref. 1. The values from counterion-only systems are set as a zero point of y-axis. To correctly illustrate the significant forking of the  $\alpha$ -carbon order parameter in PS headgroup (bottom, right), the y-axis is shifted with the same value for both order parameters such that the lower order parameter value is at zero.

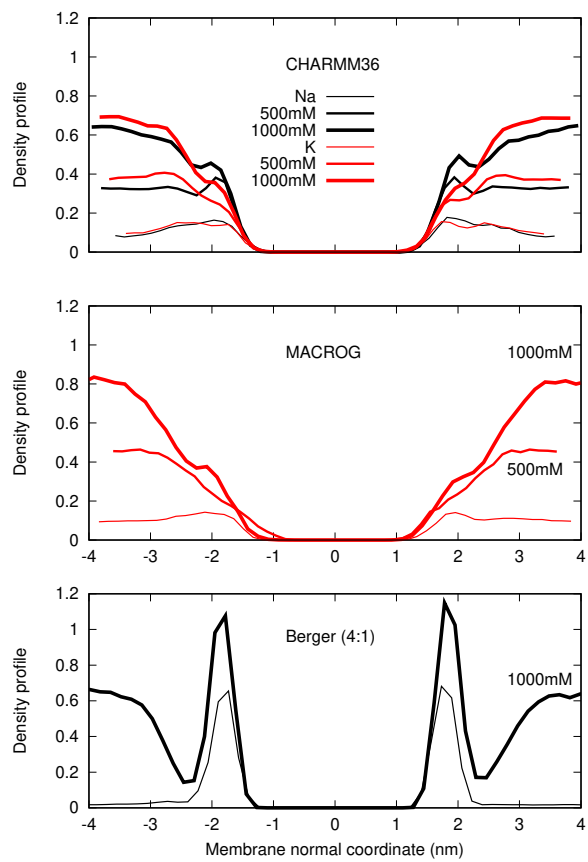


Figure S14: Counterion density distributions from PC:PS mixtures.

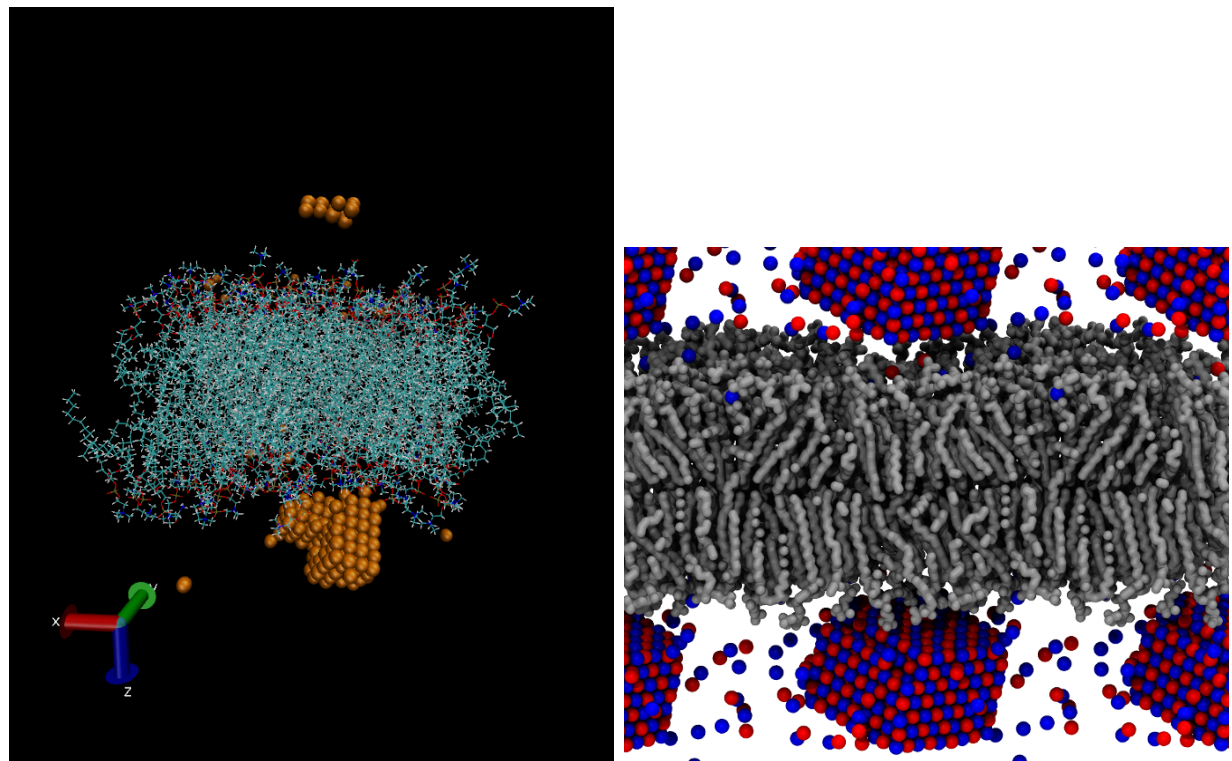


Figure S15: Ion clusters appearing in POPC:POPS (5:1) lipid17/14 simulations with 1 M of NaCl (left) and MacRog simulations with 4 M of KCl (right).

## S8 Calcium binding to POPC in CHARMM36 simulation with NBfix1 parameters

The response of POPC headgroup order parameters to the  $\text{CaCl}_2$  concentration are underestimated in simulations of POPC:POPS (5:1) mixture with CHARMM36 when employing the NBfix parameters for the interactions between calcium and lipid oxygens<sup>38,39</sup> (Fig. 9 in the main text), indicating that the calcium binding to the bilayer is too weak with these parameters. The response of headgroup order parameters (Fig. S16) and the binding affinity (Fig. S17) of calcium were underestimated also in simulations of pure POPC bilayer with the NBfix1 parameters.<sup>38</sup> Notably, CHARMM36 simulations with the NBfix1 terms<sup>3,38</sup> predict similar binding affinity for sodium and calcium. Because the results for POPC:POPS (5:1) mixture were very similar with both NBfix parameters,<sup>38,39</sup> the NBfix2 parameters were not separately tested with pure POPC bilayers. Without the NBfix parameters, the calcium binding affinity to pure POPC lipid bilayers was overestimated in the CHARMM36 model.<sup>95</sup>

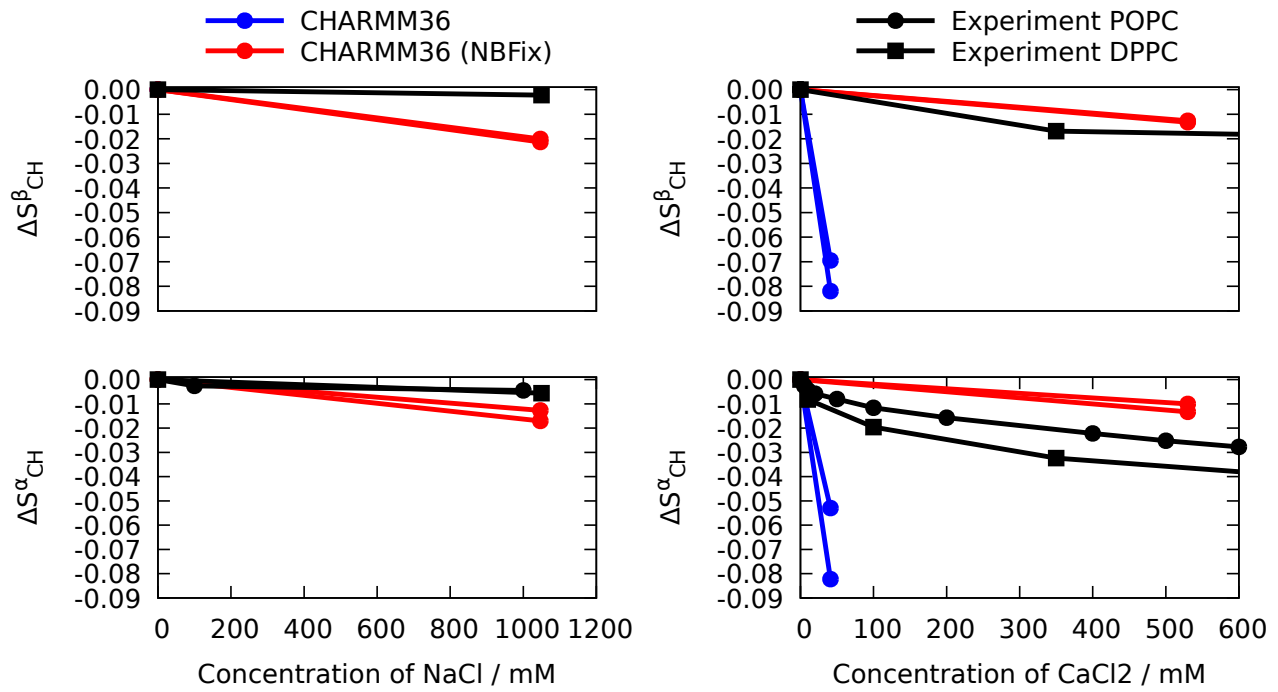


Figure S16: Headgroup order parameters from CHARMM36 simulations of POPC, where the NBfix term was employed for sodium<sup>3</sup> (*left*) and calcium<sup>38</sup> (*right*) compared with the experimental data<sup>83,84</sup> and simulations without NBfix for the calcium. Simulation files without ions are available at Ref. 106, with the NBfix term in sodium at Ref. 107, with the NBfix term in calcium at Ref. 107 and without the NBfix in calcium at Ref. 108.

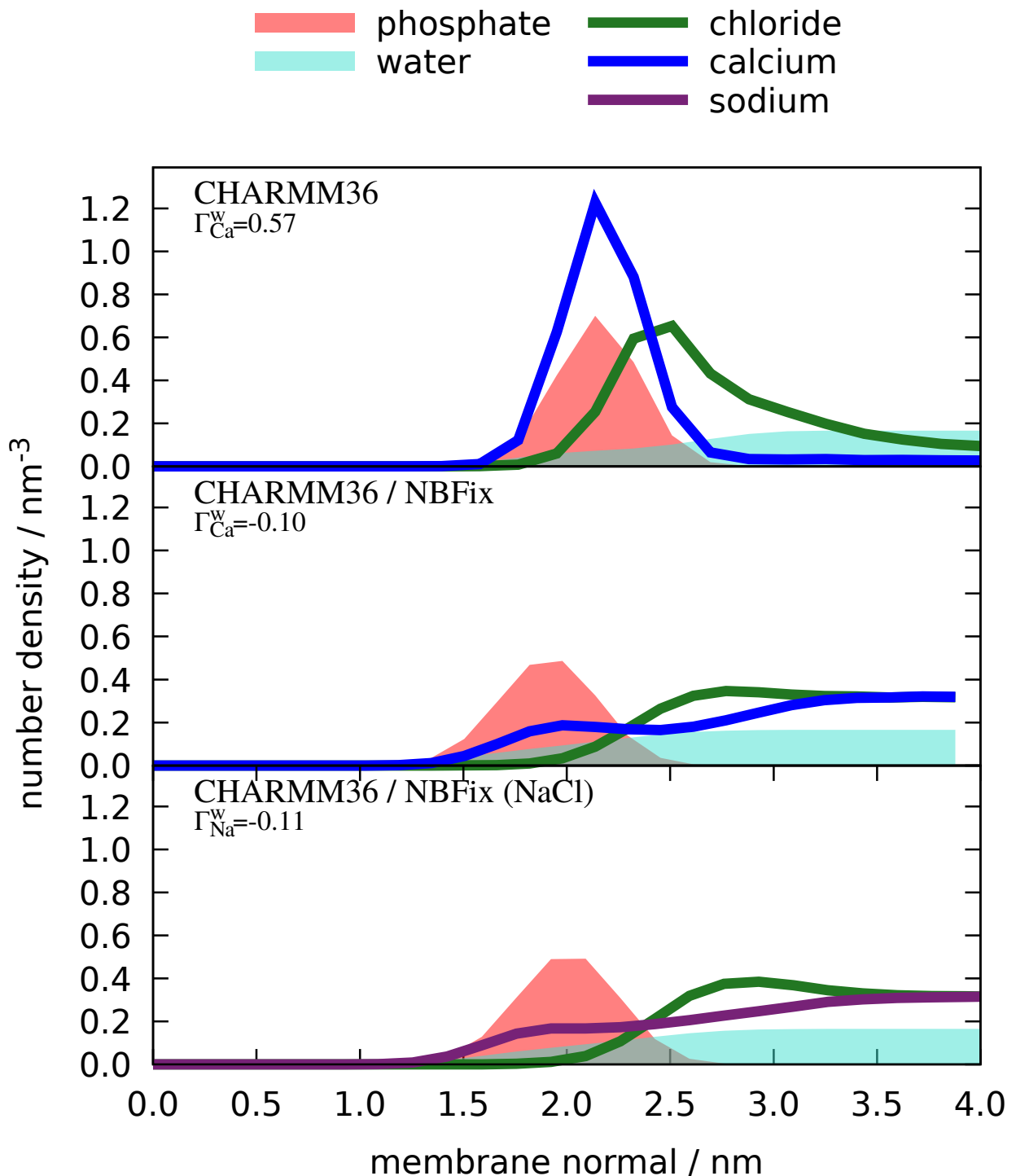


Figure S17: Density profiles along membrane normal from CHARMM36 simulations with (middle) and without (top) the NBfix term for calcium<sup>38</sup> compared to the simulation with the NBfix term for sodium<sup>3</sup> (bottom). The simulation data are the same as in Fig. S16.

## S9 Calcium density profiles from simulations with POPC:POPS(5:1) mixture

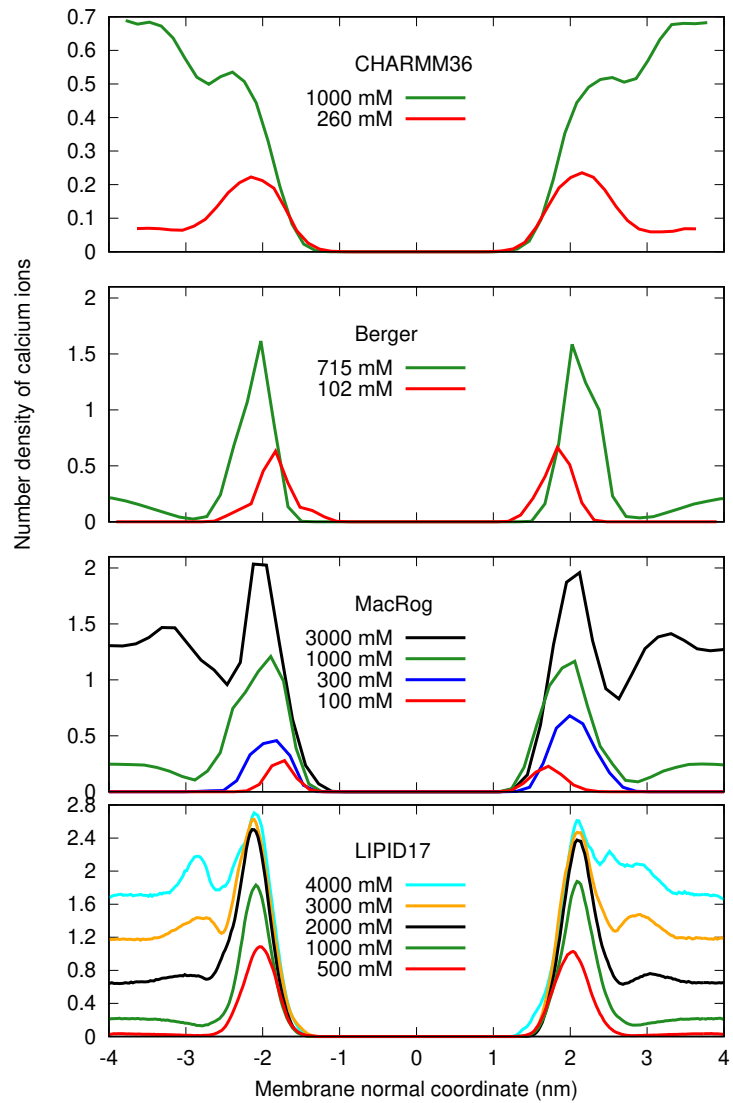


Figure S18: Number density profiles of  $\text{Ca}^{2+}$  from POPC:POPS (5:1) mixtures simulated with different force fields. The ion densities are taken along the z-axis that coincides with the bilayer normal.

## S10 Details of the force field ranking (Fig. 5)

In Figure 5 of main text we present a rough and subjective ranking of the force fields investigated in this work. The assessment was based on the data presented in Fig. 3. For each carbon (the columns in Fig. 3), we first investigated separately how well a given force field represents the **magnitude** of the order parameters and their **forking**.

### Magnitude

To quantify how close to the experimentally obtained C–H order parameters ( $S_{\text{CHS}}$ ) were to the force-field-produced  $S_{\text{CHS}}$ , we assign a number for each carbon based on the following 5-step scale:

**0 ( )**: More than half of all the calculated  $S_{\text{CHS}}$  (includes all hydrogens bound to that carbon and all lipid types investigated for the given force field) were within the *subjective sweet spots* (SSP, blue-shaded areas in Fig. 3).

**1 (m)**: All the calculated  $S_{\text{CHS}}$  were  $< 0.03$  units away from the SSP.

**2 (M)**: All the calculated  $S_{\text{CHS}}$  were  $< 0.05$  units away from the SSP.

**3 (M)**: All the calculated  $S_{\text{CHS}}$  were  $< 0.10$  units away from the SSP.

**4 (M)**: Some of the calculated  $S_{\text{CHS}}$  were  $> 0.10$  units away from the SSP.

### Forking

Forking in each force field was assessed based on how well the difference in order parameters of two hydrogens attached to a given carbon matched that obtained experimentally. Note that this is not relevant for  $\beta$  and  $g_2$ , which have only one hydrogen. For the  $\alpha$  carbon, for which a considerable forking of 0.105 is experimentally seen, the following 5-step scale was used:

**0 ( )**: The distance  $D$  between the symbols (indicating time-weighted averages in Fig. 3) was  $0.08 < D < 0.13$  units for all the calculated  $S_{\text{CHS}}$  (includes all lipid types investigated for a given force field).

**1 (F)**:  $(0.06 < D < 0.08)$  OR  $(0.13 < D < 0.15)$ .

**2 (F)**:  $(0.04 < D < 0.06)$  OR  $(0.15 < D < 0.17)$ .

**3 (F)**:  $(0.02 < D < 0.04)$  OR  $(0.17 < D < 0.19)$ .

**4 (F)**:  $(D < 0.02)$  OR  $(0.19 < D)$ .

For the  $g_3$  carbon, for which no forking is indicated by experiments, the following 5-step scale was used:

**0 ( )**:  $D < 0.02$ .

**1 (F)**:  $0.02 < D < 0.04$ .

**2 (F)**:  $0.04 < D < 0.06$ .

**3 (F)**:  $0.06 < D < 0.08$ .

**4 (F)**:  $0.08 < D$ .

For the  $g_1$  carbon, for which a considerable forking of 0.13 is experimentally seen, the following 5-step scale was used:

**0 ( )**:  $0.11 < D < 0.15$ .

**1 (F)**:  $(0.09 < D < 0.11)$  OR  $(0.15 < D < 0.17)$ .

**2 (F)**:  $(0.07 < D < 0.09)$  OR  $(0.17 < D < 0.19)$ .

**3 (F)**:  $(0.05 < D < 0.07)$  OR  $(0.19 < D < 0.21)$ .

**4 (F)**:  $(D < 0.05)$  OR  $(0.21 < D)$ .

Based on these assessments of magnitude and forking deviations from experimental values, each carbon was then assigned to one of the following groups: "within experimental error" (magnitude and forking deviations both on 0 of the scales described above), "almost within experimental error" (sum of the magnitude and forking deviation 1 or 2), "clear deviation from experiments" (sum of magnitude and forking deviation from 3 to 5), and "major deviation from experiments" (sum of magnitude and forking deviation from 6 to 8). These groups are indicated by colors in Fig. 4. (Note that for  $\beta$  and  $g_2$ , for which there can be no forking, the corresponding group assignment limits were: 0, 1, 2, and 3.)

Finally, the total ability of the force field to describe the headgroup and glycerol structure was estimated. To this end, the groups were given the following weights: 0 (within experimental error), 1 (almost within experimental error), 2 (clear deviation from experiments), 4 (major deviation from experiments), and the contributions from the five carbons were summed up. The sum, given in the  $\Sigma$ -column of Fig. 3, was then used to (roughly and subjectively) rank the force fields.

## S11 Author contributions

*Hanne Antila* contributed to the development of analysis tools used for evaluating the force fields, provided critical discussion on the manuscript content, and edited it for clarity.

*Pavel Buslaev* analysed the dihedral angle distributions in the head group and glycerol backbone regions.

*Fernando Favela-Rosales* set up and performed one of the DOPS simulations with Slipids.

*Tiago M. Ferreira* performed the NMR experiments and NMR simulations, processed and analysed the experimental data, prepared the corresponding figures, wrote parts of the manuscript (NMR methods and interpretation of the SDROSS results), and took part in the final revision.

*Ivan Gushchin* supervised the work of P.B.

*Matti Javanainen* performed most of the MacRog simulations, and provided comments on the manuscript.

*Batuhan Kav* set up, performed, and analysed Amber Lipid14/17 simulations with the Amber MD simulation package.

*Jesper J. Madsen* set up, performed, and analysed several of the CHARMM36 simulations. Provided comments on the manuscript.

*Josef Melcr* prepared tools for calculating order parameters, performed Lipid14/17 simulations with Gromacs MD simulation package, prepared the TOC figure and provided comments on the manuscript.

*Markus S. Miettinen* worked with H. A. on the analysis tools, and with B. K. on the Amber MD simulations. Made the subjective force field ranking. Edited the manuscript.

*Ricky Nencini* ran the simulations of POPC systems using CHARMM36 with and without the NB-Fix corrections, ran the simulations of POPC:POPS (5:1) systems using CHARMM36 with the NBfix2 correction, and analyzed the difference between bulk and buffer concentrations. *O. H. Samuli Ollila* designed the project and managed the work. Ran and analysed several simulations. Wrote the manuscript.

*Thomas J. Piggot* set up, performed, and analysed many of the simulations. Contributed to parts of the manuscript.

## References

- (1) Roux, M.; Bloom, M. Calcium, Magnesium, Lithium, Sodium, and Potassium Distributions in the Headgroup Region of Binary Membranes of Phosphatidylcholine and Phosphatidylserine As Seen by Deuterium NMR. *Biochemistry* **1990**, *29*, 7077–7089.
- (2) Klauda, J. B.; Venable, R. M.; Freites, J. A.; O'Connor, J. W.; Tobias, D. J.; Mondragon-Ramirez, C.; Vorobyov, I.; MacKerell Jr, A. D.; Pastor, R. W. Update of the CHARMM All-Atom Additive Force Field for Lipids: Validation on Six Lipid Types. *J. Phys. Chem. B* **2010**, *114*, 7830–7843.
- (3) Venable, R. M.; Luo, Y.; Gawrisch, K.; Roux, B.; Pastor, R. W. Simulations of Anionic Lipid Membranes: Development of Interaction-Specific Ion Parameters and Validation Using NMR Data. *J. Phys. Chem. B* **2013**, *117*, 10183–10192.
- (4) Madsen, J. J. MD Simulations of Bilayers Containing PC/PS Mixtures and CaCl<sub>2</sub>: 250POPC\_50POPS\_neutral. 2019; <https://doi.org/10.5281/zenodo.2542151>.
- (5) Piggot, T. CHARMM36 POPS/POPC Simulations (versions 1 and 2) 298 K 1.0 Nm LJ Switching with K Ions. 2018; <https://doi.org/10.5281/zenodo.1182658>.
- (6) Ollila, O. H. S. POPC:POPS (5:1) with 450 MM Potassium Simulation with CHARMM36 at 298K. 2018; <https://doi.org/10.5281/zenodo.1493241>.
- (7) Ollila, O. H. S. POPC:POPS (5:1) with 890 MM Potassium Simulation with CHARMM36 at 298K. 2018; <https://doi.org/10.5281/zenodo.1493246>.
- (8) Piggot, T. CHARMM36 POPS/POPC Simulations (versions 1 and 2) 298 K 1.0 Nm LJ Switching with Na Ions. 2018; <https://doi.org/10.5281/zenodo.1182665>.
- (9) Ollila, O. H. S. POPC:POPS (5:1) with 440 MM Sodium Simulation with CHARMM36 at 298K. 2018; <https://doi.org/10.5281/zenodo.1493190>.

- (10) Ollila, O. H. S. POPC:POPS (5:1) with 890 MM Sodium Simulation with CHARMM36 at 298K. 2018; <https://doi.org/10.5281/zenodo.1493229>.
- (11) Maciejewski, A.; Pasenkiewicz-Gierula, M.; Cramariuc, O.; Vattulainen, I.; Rög, T. Refined OPLS All-Atom Force Field for Saturated Phosphatidylcholine Bilayers at Full Hydration. *J. Phys. Chem. B* **2014**, *118*, 4571–4581.
- (12) Javanainen, M. Simulations of POPC/POPS Membranes with CaCl<sub>2</sub>. 2017; <https://doi.org/10.5281/zenodo.1409551>.
- (13) Javanainen, M. Simulations of POPC/POPS Membranes with KCl. 2018; <https://doi.org/10.5281/zenodo.1404040>.
- (14) Dickson, C. J.; Madej, B. D.; Skjevik, A. A.; Betz, R. M.; Teigen, K.; Gould, I. R.; Walker, R. C. Lipid14: The Amber Lipid Force Field. *J. Chem. Theory Comput.* **2014**, *10*, 865–879.
- (15) Gould, I.; Skjevik, A.; Dickson, C.; Madej, B.; Walker, R. Lipid17: A Comprehensive AMBER Force Field for the Simulation of Zwitterionic and Anionic Lipids. 2018; In preparation.
- (16) Kav, B.; Miettinen, M. S. Amber Lipid17 Simulations of POPC/POPS Membranes with KCl Counterions. 2018; <https://doi.org/10.5281/zenodo.1250969>.
- (17) Kav, B.; Miettinen, M. S. Amber Lipid17 Simulations of POPC/POPS Membranes with KCl. 2018; <https://doi.org/10.5281/zenodo.1227257>.
- (18) Kav, B.; Miettinen, M. S. Amber Lipid17 Simulations of POPC/POPS Membranes with NaCl Counterions. 2018; <https://doi.org/10.5281/zenodo.1250975>.
- (19) Kav, B.; Miettinen, M. S. Amber Lipid17 Simulations of POPC/POPS Membranes with NaCl. 2018; <https://doi.org/10.5281/zenodo.1227272>.

- (20) Tieleman, D. P.; Berendsen, H. J.; Sansom, M. S. an Alamethicin Channel in a Lipid Bilayer: Molecular Dynamics Simulations. *Biophys. J.* **1999**, *76*, 1757 – 1769.
- (21) Mukhopadhyay, P.; Monticelli, L.; Tieleman, D. P. Molecular Dynamics Simulation of a Palmitoyl-Oleoyl Phosphatidylserine Bilayer with Na<sup>+</sup> Counterions and NaCl. *Biophys. J.* **2004**, *86*, 1601 – 1609.
- (22) Ollila, O. H. S. POPC:POPS (4:1) Simulation with Berger Model at 310K. 2018; <https://doi.org/10.5281/zenodo.1475285>.
- (23) Cwiklik, L. MD Simulation Trajectory of a POPC/POPS (4:1) Bilayer with 1M NaCl, Berger Force Field for Lipids and Ffgmx for Ions. 2017; <https://doi.org/10.5281/zenodo.838219>.
- (24) Botan, A.; Favela-Rosales, F.; Fuchs, P. F. J.; Javanainen, M.; Kanduč, M.; Kulig, W.; Lamberg, A.; Loison, C.; Lyubartsev, A.; Miettinen, M. S. et al. Toward Atomistic Resolution Structure of Phosphatidylcholine Headgroup and Glycerol Backbone at Different Ambient Conditions. *J. Phys. Chem. B* **2015**, *119*, 15075–15088.
- (25) Fernando, F.-R. POPC\_Glycerol\_CHARMM36\_0-10-15-20-25-35-50%CHOL. 2015; <http://dx.doi.org/10.5281/zenodo.16830>, Because of the system size, the files ONLY contain the coordinates of Glycerol saved every 10ps, this is the real contribution to the nmrlipids project.
- (26) Lee, J.; Cheng, X.; Swails, J. M.; Yeom, M. S.; Eastman, P. K.; Lemkul, J. A.; Wei, S.; Buckner, J.; Jeong, J. C.; Qi, Y. et al. CHARMM-GUI Input Generator for NAMD, GROMACS, AMBER, OpenMM, and CHARMM/OpenMM Simulations Using the CHARMM36 Additive Force Field. *J. Chem. Theory Comput.* **2016**, *12*, 405–413.
- (27) Jo, S.; Kim, T.; Iyer, V. G.; Im, W. CHARMM-GUI: A Web-Based Graphical User Interface for CHARMM. *J. Comput. Chem.* **29**, 1859–1865.

- (28) Durell, S. R.; Brooks, B. R.; Ben-Naim, A. Solvent-Induced Forces Between Two Hydrophilic Groups. *The Journal of Physical Chemistry* **1994**, *98*, 2198–2202.
- (29) Neria, E.; Fischer, S.; Karplus, M. Simulation of Activation Free Energies in Molecular Systems. *J. Chem. Phys.* **1996**, *105*, 1902–1921.
- (30) Abraham, M. J.; Murtola, T.; Schulz, R.; Páll, S.; Smith, J. C.; Hess, B.; Lindahl, E. GROMACS: High Performance Molecular Simulations Through Multi-Level Parallelism from Laptops to Supercomputers. *SoftwareX* **2015**, *1*, 19–25.
- (31) Hess, B.; Bekker, H.; Berendsen, H. J. C.; Fraaije, J. G. E. M. LINCS: a linear constraint solver for molecular dynamics simulations. *J. Comput. Chem.* **1997**, *18*, 1463–1472.
- (32) Hess, B. P-LINCS: A Parallel Linear Constraint Solver for Molecular Simulation. *J. Chem. Theory Comput.* **2008**, *4*, 116–122.
- (33) Nose, S. A molecular dynamics method for simulations in the canonical ensemble. *Mol. Phys.* **1984**, *52*, 255–268.
- (34) Hoover, W. G. Canonical dynamics: Equilibrium phase-space distributions. *Phys. Rev. A* **1985**, *31*, 1695–1697.
- (35) Parrinello, M.; Rahman, A. Polymorphic transitions in single crystals: A new molecular dynamics method. *J. Appl. Phys.* **1981**, *52*, 7182–7190.
- (36) Darden, T.; York, D.; Pedersen, L. Particle Mesh Ewald: An  $N \cdot \log(N)$  Method for Ewald Sums in Large Systems. *J. Chem. Phys.* **1993**, *98*, 10089–10092.
- (37) Essman, U. L.; Perera, M. L.; Berkowitz, M. L.; Larden, T.; Lee, H.; Pedersen, L. G. A smooth particle mesh ewald potential. *J. Chem. Phys.* **1995**, *103*, 8577–8592.
- (38) Kim, S.; Patel, D. S.; Park, S.; Slusky, J.; Klauda, J. B.; Widmalm, G.; Im, W. Bilayer Properties of Lipid a from Various Gram-Negative Bacteria. *Biophys. J.* **2016**, *111*, 1750 – 1760.

- (39) Han, K.; Venable, R. M.; Bryant, A.-M.; Legacy, C. J.; Shen, R.; Li, H.; Roux, B.; Gericke, A.; Pastor, R. W. Graph-Theoretic Analysis of Monomethyl Phosphate Clustering in Ionic Solutions. *The Journal of Physical Chemistry B* **2018**, *122*, 1484–1494.
- (40) Lee, S.; Tran, A.; Allsopp, M.; Lim, J. B.; Henin, J.; Klauda, J. B. CHARMM36 United Atom Chain Model for Lipids and Surfactants. *J. Phys. Chem. B* **2014**, *118*, 547–556.
- (41) Kulig, W.; Pasenkiewicz-Gierula, M.; Róg, T. Topologies, Structures and Parameter Files for Lipid Simulations in GROMACS with the OPLS-Aa Force Field: DPPC, POPC, DOPC, PEPC, and Cholesterol. *Data in Brief* **2015**, *5*, 333 – 336.
- (42) Kulig, W.; Pasenkiewicz-Gierula, M.; Róg, T. Cis and Trans Unsaturated Phosphatidyl-choline Bilayers: A Molecular Dynamics Simulation Study. *Chem. Phys. Lipids* **2016**, *195*, 12 – 20.
- (43) Jorgensen, W. L.; Chandrasekhar, J.; Madura, J. D.; Impey, R. W.; Klein, M. L. Comparison of Simple Potential Functions for Simulating Liquid Water. *J. Chem. Phys.* **1983**, *79*, 926–935.
- (44) Javanainen, M. Simulation of a POPC Bilayer at 298K, Lipid Model by Maciejewski and Rog. 2018; <https://doi.org/10.5281/zenodo.1167532>.
- (45) Róg, T.; Orłowski, A.; Llorente, A.; Skotland, T.; Sylvänen, T.; Kauhanen, D.; Ekroos, K.; Sandvig, K.; Vattulainen, I. Data Including GROMACS Input Files for Atomistic Molecular Dynamics Simulations of Mixed, Asymmetric Bilayers Including Molecular Topologies, Equilibrated Structures, and Force Field for Lipids Compatible with OPLS-Aa Parameters. *Data in Brief* **2016**, *7*, 1171 – 1174.
- (46) Javanainen, M. Simulation of a POPS Membrane with Potassium Counterions. 2018; <https://doi.org/10.5281/zenodo.1434990>.

- (47) Páll, S.; Hess, B. a Flexible Algorithm for Calculating Pair Interactions on {SIMD} Architectures. *Comput. Phys. Commun.* **2013**, *184*, 2641 – 2650.
- (48) Åqvist, J. Ion-Water Interaction Potentials Derived from Free Energy Perturbation Simulations. *J. Phys. Chem.* **1990**, *94*, 8021–8024.
- (49) Shirts, M. R.; Mobley, D. L.; Chodera, J. D.; Pande, V. S. Accurate and Efficient Corrections for Missing Dispersion Interactions in Molecular Simulations. *J. Phys. Chem. B* **2007**, *111*, 13052–13063.
- (50) Miyamoto, S.; Kollman, P. A. SETTLE: An analytical Version of the SHAKE and RATTLE Algorithm for Rigid Water Models. *J. Comput. Chem* **1992**, *13*, 952–962.
- (51) Jorgensen, W. L.; Chandrasekhar, J.; Madura, J. D.; Impey, R. W.; Klein, M. L. Comparison of Simple Potential Functions for Simulating Liquid Water. *The Journal of chemical physics* **1983**, *79*, 926–935.
- (52) Case, D.; Ben-Shalom, I.; Brozell, S.; Cerutti, D.; T.E. Cheatham, I.; Cruzeiro, V.; Darden, T.; Duke, R.; Ghoreishi, D.; Gilson, M. et al. AMBER 2018. 2018.
- (53) Joung, I. S.; Cheatham III, T. E. Determination of Alkali and Halide Monovalent Ion Parameters for Use in Explicitly Solvated Biomolecular Simulations. *The journal of physical chemistry B* **2008**, *112*, 9020–9041.
- (54) Miettinen, M. S.; Kav, B. Molecular Dynamics Simulation Trajectory of an Anionic Lipid Bilayer: 100 Mol% POPC with Na<sup>+</sup> Counterions Using Joung-Cheatham Ions. 2018; <https://doi.org/10.5281/zenodo.1148495>.
- (55) Miettinen, M. S.; Kav, B. Molecular Dynamics Simulation Trajectory of an Anionic Lipid Bilayer: 100 Mol% POPC with Na<sup>+</sup> Counterions Using Ff99 Ions. 2018; <https://doi.org/10.5281/zenodo.1134869>.

- (56) Kav, B.; Miettinen, M. S. Molecular Dynamics Simulation Trajectory of an Anionic Lipid Bilayer: 100 Mol% DOPS with Na+ Counterions Using Joung-Cheetham Ions. 2018; <https://doi.org/10.5281/zenodo.1134871>.
- (57) Kav, B.; Miettinen, M. S. Molecular Dynamics Simulation Trajectory of an Anionic Lipid Bilayer: 100 Mol% DOPS with Na+ Counterions Using Ff99 Ions. 2018; <https://doi.org/10.5281/zenodo.1135142>.
- (58) Kav, B.; Miettinen, M. S. Amber Lipid17 Simulations of POPC/POPS Membranes with CaCl<sub>2</sub>. 2018; <https://doi.org/10.5281/zenodo.1438848>.
- (59) Sousa da Silva, A.; Vranken, W. ACPYPE - AnteChamber PYthon Parser interfacE. *BMC Research Notes* **2012**, *5*, 367.
- (60) Ollila, O. H. S.; Retegan, M. MD Simulation Trajectory and Related Files for POPC Bilayer (Lipid14, Gromacs 4.5). 2014; <http://dx.doi.org/10.5281/zenodo.12767>.
- (61) Smith, D. E.; Dang, L. X. Computer Simulations of NaCl Association in Polarizable Water. *J. Chem. Phys* **1994**, *100*, 3757–3766.
- (62) Dang, L. X.; Schenter, G. K.; Glezakou, V.-A.; Fulton, J. L. Molecular Simulation Analysis and X-Ray Absorption Measurement of Ca<sup>2+</sup>, K<sup>+</sup> and Cl<sup>-</sup> Ions in Solution. *J. Phys. Chem. B* **2006**, *110*, 23644–54.
- (63) Bussi, G.; Donadio, D.; Parrinello, M. Canonical Sampling Through Velocity Rescaling. *J. Chem. Phys.* **2007**, *126*.
- (64) Melcr, J. Molecular Dynamics Simulations of Lipid Bilayers Containing POPC and POPS with the Lipid17 Force Field, Only Counterions, and CaCl<sub>2</sub> Concentrations. 2018; <https://doi.org/10.5281/zenodo.1487761>.
- (65) Melcr, J.; Ferreira, T.; Jungwirth, P.; Ollila, O. H. S. Improved Cation Binding to Lipid Bilayer with Negatively Charged POPS by Effective Inclu-

- sion of Electronic Polarization. [https://github.com/ohsOllila/ecc\\_lipids/blob/master/Manuscript/manuscript.pdf](https://github.com/ohsOllila/ecc_lipids/blob/master/Manuscript/manuscript.pdf), Submitted.
- (66) Jämbeck, J. P. M.; Lyubartsev, A. P. Implicit Inclusion of Atomic Polarization in Modeling of Partitioning Between Water and Lipid Bilayers. *Phys. Chem. Chem. Phys.* **2013**, *15*, 4677–4686.
- (67) Jämbeck, J. P.; Lyubartsev, A. P. Another Piece of the Membrane Puzzle: Extending Slipids Further. *Journal of chemical theory and computation* **2012**, *9*, 774–784.
- (68) Wennberg, C. L.; Murtola, T.; Páll, S.; Abraham, M. J.; Hess, B.; Lindahl, E. Direct-Space Corrections Enable Fast and Accurate Lorentz–Berthelot Combination Rule Lennard-Jones Lattice Summation. *J. Chem. Theory Comput.* **2015**, *11*, 5737–5746.
- (69) Ghahremanpour, M. M.; Arab, S. S.; Aghazadeh, S. B.; Zhang, J.; van der Spoel, D. MemBuilder: A Web-Based Graphical Interface to Build Heterogeneously Mixed Membrane Bilayers for the GROMACS Biomolecular Simulation Program. *Bioinformatics* **2013**, *30*, 439–441.
- (70) Ollila, S.; Hyvönen, M. T.; Vattulainen, I. Polyunsaturation in Lipid Membranes: Dynamic Properties and Lateral Pressure Profiles. *J. Phys. Chem. B* **2007**, *111*, 3139–3150.
- (71) Ollila, O. H. S. MD Simulation of POPC Lipids Bilayer at 310K (Berger, Gromacs 3.1.4). 2018; <https://doi.org/10.5281/zenodo.1230170>.
- (72) Berendsen, H. J. C.; Postma, J. P. M.; van Gunsteren, W. F.; Hermans, J. In *Intermolecular Forces*; Pullman, B., Ed.; Reidel: Dordrecht, 1981; Chapter Interaction models for water in relation to protein hydration, pp 331–342.
- (73) Jurkiewicz, P.; Cwiklik, L.; Vojtíšková, A.; Jungwirth, P.; Hof, M. Structure, Dynamics,

and Hydration of POPC/POPS Bilayers Suspended in NaCl, KCl, and CsCl Solutions.

*Biochim. Biophys. Acta* **2012**, *1818*, 609 – 616.

- (74) Melcrová, A.; Pokorna, S.; Pullanchery, S.; Kohagen, M.; Jurkiewicz, P.; Hof, M.; Jungwirth, P.; Cremer, P. S.; Cwiklik, L. the Complex Nature of Calcium Cation Interactions with Phospholipid Bilayers. *Sci. Reports* **2016**, *6*, 38035.
- (75) Cwiklik, L. MD Simulation Trajectory of a POPC/POPS (4:1) Bilayer with 102mM CaCl<sub>2</sub>, Berger Force Field for Lipids, Scaled Charges for Ca<sup>2+</sup> and Cl<sup>-</sup>. 2017; <https://doi.org/10.5281/zenodo.887398>.
- (76) Cwiklik, L. MD Simulation Trajectory of a POPC/POPS (4:1) Bilayer with 715mM CaCl<sub>2</sub>, Berger Force Field for Lipids, Scaled Charges for Ca<sup>2+</sup> and Cl<sup>-</sup>. 2017; <https://doi.org/10.5281/zenodo.887400>.
- (77) Chandrasekhar, I.; Kastenholz, M.; Lins, R.; Oostenbrink, C.; Schuler, L.; Tieleman, D.; Gunsteren, W. A Consistent Potential Energy Parameter Set for Lipids: Dipalmitoylphosphatidylcholine As a Benchmark of the GROMOS96 45A3 Force Field. *Eur. Biophys. J.* **2003**, *32*, 67–77.
- (78) Kukol, A. Lipid Models for United-Atom Molecular Dynamics Simulations of Proteins. *J. Chem. Theory Comput.* **2009**, *5*, 615–626.
- (79) Piggot, T. J.; Piñeiro, Á.; Khalid, S. Molecular Dynamics Simulations of Phosphatidyl-choline Membranes: A Comparative Force Field Study. *J. Chem. Theory Comput.* **2012**, *8*, 4593–4609.
- (80) Piggot, T. J.; Holdbrook, D. A.; Khalid, S. Electroporation of the E. Coli and S. Aureus Membranes: Molecular Dynamics Simulations of Complex Bacterial Membranes. *J. Phys. Chem. B* **2011**, *115*, 13381–13388.

- (81) Holdbrook, D. A.; Leung, Y. M.; Piggot, T. J.; Marius, P.; Williamson, P. T. F.; Khalid, S. Stability and Membrane Orientation of the Fukutin Transmembrane Domain: A Combined Multiscale Molecular Dynamics and Circular Dichroism Study. *Biochemistry* **2010**, *49*, 10796–10802.
- (82) Schmid, N.; Eichenberger, A. P.; Choutko, A.; Riniker, S.; Winger, M.; Mark, A. E.; van Gunsteren, W. F. Definition and Testing of the GROMOS Force-Field Versions 54A7 and 54B7. *Eur. Biophys. J.* **2011**, *40*, 843.
- (83) Akutsu, H.; Seelig, J. Interaction of Metal Ions with Phosphatidylcholine Bilayer Membranes. *Biochemistry* **1981**, *20*, 7366–7373.
- (84) Altenbach, C.; Seelig, J. Calcium Binding to Phosphatidylcholine Bilayers As Studied by Deuterium Magnetic Resonance. Evidence for the Formation of a Calcium Complex with Two Phospholipid Molecules. *Biochemistry* **1984**, *23*, 3913–3920.
- (85) Seelig, J.; MacDonald, P. M.; Scherer, P. G. Phospholipid Head Groups As Sensors of Electric Charge in Membranes. *Biochemistry* **1987**, *26*, 7535–7541.
- (86) Scherer, P. G.; Seelig, J. Electric Charge Effects on Phospholipid Headgroups. Phosphatidylcholine in Mixtures with Cationic and Anionic Amphiphiles. *Biochemistry* **1989**, *28*, 7720–7728.
- (87) Borle, F.; Seelig, J. Ca<sup>2+</sup> Binding to Phosphatidylglycerol Bilayers As Studied by Differential Scanning Calorimetry and <sup>2</sup>H- and <sup>31</sup>P-Nuclear Magnetic Resonance. *Chem. Phys. Lipids* **1985**, *36*, 263 – 283.
- (88) Macdonald, P. M.; Seelig, J. Calcium Binding to Mixed Phosphatidylglycerol-Phosphatidylcholine Bilayers As Studied by Deuterium Nuclear Magnetic Resonance. *Biochemistry* **1987**, *26*, 1231–1240.

- (89) Roux, M.; Neumann, J.-M. Deuterium NMR Study of Head-Group Deuterated Phosphatidylserine in Pure and Binary Phospholipid Bilayers. *FEBS Letters* **1986**, *199*, 33–38.
- (90) Roux, M.; Bloom, M. Calcium Binding by Phosphatidylserine Headgroups. Deuterium NMR Study. *Biophys. J.* **1991**, *60*, 38 – 44.
- (91) Scherer, P.; Seelig, J. Structure and Dynamics of the Phosphatidylcholine and the Phosphatidylethanolamine Head Group in L-M Fibroblasts As Studied by Deuterium Nuclear Magnetic Resonance. *EMBO J.* **1987**, *6*.
- (92) Ferreira, T. M.; Coreta-Gomes, F.; Ollila, O. H. S.; Moreno, M. J.; Vaz, W. L. C.; Topgaard, D. Cholesterol and POPC Segmental Order Parameters in Lipid Membranes: Solid State  $^1\text{H}$ - $^{13}\text{C}$  NMR and MD Simulation Studies. *Phys. Chem. Chem. Phys.* **2013**, *15*, 1976–1989.
- (93) Ollila, O. S.; Pabst, G. Atomistic Resolution Structure and Dynamics of Lipid Bilayers in Simulations and Experiments. *Biochim. Biophys. Acta* **2016**, *1858*, 2512 – 2528.
- (94) Ferreira, T. M.; Sood, R.; Bärenwald, R.; Carlström, G.; Topgaard, D.; Saalwächter, K.; Kinnunen, P. K. J.; Ollila, O. H. S. Acyl Chain Disorder and Azelaoyl Orientation in Lipid Membranes Containing Oxidized Lipids. *Langmuir* **2016**, *32*, 6524–6533.
- (95) Catte, A.; Girych, M.; Javanainen, M.; Loison, C.; Melcr, J.; Miettinen, M. S.; Monticelli, L.; Maatta, J.; Oganesyan, V. S.; Ollila, O. H. S. et al. Molecular Electrometer and Binding of Cations to Phospholipid Bilayers. *Phys. Chem. Chem. Phys.* **2016**, *18*, 32560–32569.
- (96) Melcr, J.; Martinez-Seara, H.; Nencini, R.; Kolafa, J.; Jungwirth, P.; Ollila, O. H. S. Accurate Binding of Sodium and Calcium to a POPC Bilayer by Effective Inclusion of Electronic Polarization. *J. Phys. Chem. B* **2018**, *122*, 4546–4557.

- (97) Ollila, O. H. S. CHARMM36 Simulations of POPC Mixed with Cationic Surfactant. 2018; <https://doi.org/10.5281/zenodo.1288297>.
- (98) Dvinskikh, S. V.; Zimmermann, H.; Maliniak, A.; Sandstrom, D. Measurements of Motionally Averaged Heteronuclear Dipolar Couplings in MAS NMR Using R-Type Recoupling. *J. Magn. Reson.* **2004**, *168*, 194–201.
- (99) Browning, J. L.; Seelig, J. Bilayers of Phosphatidylserine: A Deuterium and Phosphorus Nuclear Magnetic Resonance Study. *Biochemistry* **1980**, *19*, 1262–1270.
- (100) Melcr, J. POPC Lipid Membrane, 303K, Charmm36 Force Field, Simulation Files and 200 Ns Trajectory for Gromacs MD Simulation Engine V5.1.2. 2016; <https://doi.org/10.5281/zenodo.153944>.
- (101) Favela-Rosales, F. MD Simulation Trajectory of a Lipid Bilayer: Pure POPC in Water. SLIPIDS, Gromacs 4.6.3. 2016. 2016; <https://doi.org/10.5281/zenodo.166034>.
- (102) Hauser, H.; Shipley, G. G. Interactions of Monovalent Cations with Phosphatidylserine Bilayer Membranes. *Biochemistry* **1983**, *22*, 2171–2178.
- (103) Hauser, H.; Shipley, G. Comparative Structural Aspects of Cation Binding to Phosphatidylserine Bilayers. *Biochim. Biophys. Acta* **1985**, *813*, 343 – 346.
- (104) Mattai, J.; Hauser, H.; Demel, R. A.; Shipley, G. G. Interactions of Metal Ions with Phosphatidylserine Bilayer Membranes: Effect of Hydrocarbon Chain Unsaturation. *Biochemistry* **1989**, *28*, 2322–2330.
- (105) Cevc, G. Membrane Electrostatics. *Biochim. Biophys. Acta* **1990**, *1031*, 311 – 382.
- (106) Nencini, R. Simulation Data for CHARMM36 POPC Bilayer, 100 Lipids/leaflet, 310K, GROMACS 5.1.4. 2018; <https://doi.org/10.5281/zenodo.1198158>.

- (107) Nencini, R. Simulation Data for CHARMM36 POPC Bilayer, 100 Lipids/leaflet, 450 MM CaCl<sub>2</sub> ("NB-Fix" Used), 310K, GROMACS 5.1.4. 2018; <https://doi.org/10.5281/zenodo.1198171>.
- (108) Javanainen, M. POPC @ 310K, 450 MM of CaCl<sub>2</sub>. Charmm36 with Default Charmm Ions. 2016; <http://dx.doi.org/10.5281/zenodo.51185>.